REAL TIME FLOOD FORECASTING OF BAGMATI RIVER BASIN IN NEPAL

A DISSERTATION

Submitted in partial fulfillment of the

Requirements for the award of the degree

of

MASTER OF TECHNOLOGY

in

WATER RESOURCES DEVELOPMENT

(CIVIL)

By

JAMUNA PARIYAR
(17548007)

DEPARTMENT OF WATER RESOURCES DEVELOPMENT AND MANAGEMENT

INDIAN INSTITUTE OF TECHNOLOGY ROORKEE

ROORKEE-247667, UTTARAKHAND (INDIA)

MAY, 2019

INDIAN INSTITUTE OF TECHNOLOGY ROORKEE

CANDIDATE'S DECLARATION

I hereby declare that the work which is being presented in the dissertation, entitled "**REAL TIME FLOOD FORECASTING OF BAGMATI RIVER BASIN IN NEPAL"**, in the partial fulfilment of the requirements for the award of the Degree of Master of Technology in Water Resources Development and submitted in the Department of Water Resources Development and Management of the Indian Institute of Technology, Roorkee, is an authentic record of my own work carried out during the period from July 2018 to May 2019 under the supervision of Prof. S. K. Mishra and Prof. R.D. Singh, Department of Water Resources Development and Management, Roorkee, Uttarakhand, India.

The matter presented in this dissertation report has not been submitted by me for the award of any other degree in this or any other Institute.

Date: May 2019 Jamuna Pariyar

Place: WRD&M, IIT Roorkee. Enrolment No. 17548007

CERTIFICATE

This is to certify that the above statement made by the candidate is correct to the best of our knowledge.

Prof. R.D. Singh Prof. S.K. Mishra

Department of Water Resource Development & Management,
Indian Institute of Technology Roorkee, India

ACKNOWLEDGEMENT

It is my sincere appreciation to my supervisors Prof. S.K. Mishra, and Prof. R. D. Singh, Department of Water Resources Development and Management, IIT Roorkee for their valuable guidance, constant encouragement, support and co-operation for ongoing dissertation on "Real Time Flood Forecasting of Bagmati River Basin in Nepal". I am greatly obliged for their continued efforts throughout the work. Working under their guidance is a privilege and an excellent learning experience that I will cherish life time.

I am also very much thankful to Dr M.L Kansal, Professor & Head, Dr. Deepak Khare, Professor, Dr. Ashish Pandey, Associate Professor and Dr. T. R Chelliah, Associate Professor, in the Department of Water Resources Development and Management (WRD&M) for instructing and sharing in-depth knowledge in water resources sector.

I am also very much grateful to my parent organization "Ministry of Energy, Water Resources and Irrigation Nepal and Government of India (ITEC Program) for sponsoring me for M. Tech. (WRD) course at Dept. of WRDM, IIT Roorkee.

Finally, I am especially appreciative to each one of my cohorts and my family members for their continuous inspiration, support and affection throughout the study period.

(Jamuna Pariyar)

Enrolment No 17548007

ABSTRACT

Bagmati River Basin of Nepal is subjected to frequent flooding even washing away of the water level gauging stations. Estimation of surface runoff in the basin due to precipitation and quantifying discharge at desired location is important aspect of flood forecasting and management plan. The study area of Bagmati River Basin has been taken up to Bhorleni gauging site having the catchment area of 1694 sq.km. In this study, HEC-HMS hydrological model of version 4.2.1 is used to simulate rainfall-runoff process and the basin is taken as the single basin. The Arc Map-Arc-GIS version 10.4.1 and HEC-GeoHMS version 4.2 are used to process different types of spatial data required as input for the HEC-HMS model applications. All temporal data required for running HEC-HMS model are processed and utilized as input in the prescribed format required for the model. The model is applied with recession method for base flow estimation and initial and constant rate method for loss model. Two different transform methods viz. Clark and Snyder transform model are used in the study. Model is calibrated and validated using the available hourly rainfall and runoff data of three storm events observed in flood season of year 2018. The model is calibrated with two storm events and validated with one storm event by comparing observed and simulated discharges at the Bhorleni gauging site. Various performance criteria viz. peak value, total volume generated and Nash-Sutcliffe efficiency are used for evaluating the models. NSE values obtained from the Clark and Snyder transform models are 0.791 and 0.755 respectively. Comparison of result of Clark with Snyder shows that Clark method is more satisfactory in terms of higher Nash-Sutcliffe Efficiency. The calibrated and validated Clark model yielded 16.59% of error in peak, 25.00% of error in time to peak and 1.68% error in discharge volume. The results show the suitability of HEC-HMS in simulating rainfall-runoff process of Bagmati River Basin. Further, the validated storm event is used to generate unit hydrograph for Bagmati river basin for flood forecasting.

The representative unit hydrograph for the basin derived from the Clark's model is applied for formulation of the real time flood forecast for the event of 11 July 2018-14 July 2018, considering the blocks of hourly excess rainfall available up to the period of forecast. The peak discharge of the forecasted unit hydrograph for different block periods have been derived. While comparing, it is observed that the forecasted flood hydrographs slightly fit the observed flood hydrograph.

Using the developed error prediction model based on multiple linear regression approach, real time flood forecast has been updated. The flood forecast updated using the developed model for the error is based on the past observation and simulation result. The updated flood forecast significantly improved as it is very close to the observed flood hydrograph.

TABLE OF CONTENTS

Contents **Page**

LIST OF TABLES

Description of Tables **Page No.**

LIST OF FIGURES

Description of Figures **Page No.**

LIST OF ACRONYMS AND ABBREVIATIONS

ArcGIS	Aeronautical Reconnaissance Coverage Geographical Information System
ANN	Artificial Neural Network
DEM	Digital Elevation Model
DHM	Department of Hydrology and Meteorology
DRH	Direct Runoff Hydrograph
Et al.	and others (from the Latin et alii)
FAO	Food and Agriculture Organization
GLOF	Glacial Lake Outburst Flood
Ha	Hectares
HEC-GeoHMS	Hydrologic Energy Center – Geospatial Hydrologic Modeling
HEC-HMS	Hydrologic Engineering Center – Hydrologic Modeling System
ICHARM	International Centre for Water Hazard and Risk Management
ICIMOD	The international Centre for Integrated Mountain Development
IDW	Inverse Weighted Distance
i.e.	that is (from the Latin id est)
IUH	Instantaneous Unit Hydrograph
km	Kilometers
m^3/sec	Cubic Meter per Second
MSL	Mean Sea Level
NSE	Nash – Sutcliffe Efficiency
SRTM	Shuttle Radar Topographic Mission
UH	Unit Hydrograph
UNDP	United Nations Development Programme
USACE	United States Army Corps of Engineers
USGS	United States Geographical Survey

CHAPTER 1. INTRODUCTION

1.1 BACKGROUND

Precipitation is highly concentrated in the monsoon season in Nepal. About 75 percent precipitation occurs in monsoon (June-September) (Pokhrel 2004). The flood phenomenon is common in the rainy season. Due to the high concentration of monsoon, high relief, steep mountain topography and deep and narrow river valleys with frequent mass wasting phenomena renders the country more hazardous and losses more property and human life annually. Every year about Rs. 748.95 million has been lost due to water induced disaster in Nepal (Pokhrel 2004). The overall development of the country has been severely affected by repeated flooding. In the context of recent global warming phenomena, the probability and potentially damaging of flood is likely to increase with a consequent increase in the intensity of extreme precipitation events and the dynamic of glacial lakes in high mountain areas.

Nepal lies at the central part of the Hindu-Kush Himalayan belt having an area of 147,181 sq. km. between India and China. The elevation of the country ranges from 60m at Terai (Jhapa) to 8848m at Mt. Everest in the north. The average annual precipitation is around 1600mm. There are about 6000 rivers and rivulets drain in Nepal. Nepal suffers from various types of water-induced disasters such as soil erosion, landslides, debris flow, flood, bank erosion etc. due to its rocky topographically, weak geological formations, active seismic conditions, occasional glacier lake outburst floods, concentrated monsoon rains associated with unscientific land utilizations.

Floods are the most common natural disasters occurring in various parts of the world. More than one third of the world's land is prone to flood affecting around 82 percentage of the total population (Dilley et al., 2005). Around 196 million individual in more than 90 countries are exposed to catastrophic flooding, and that somewhere in the range of 170,000 deaths were connected with floods worldwide between 1980 and 2000 (UNDP, 2004). These figures portray that flooding is a major concern in many places of the world. Globally, the economic cost of extreme weather events and flood disasters is severed, and if it rises due to climate change, it will hit poorest nations the hardest consequently; the poorest section of people will bear the brunt of it. It has been reported that there has been

increase in number of major flood disasters in the world in recent period. There were six in the 1950s; seven in the 1960s; eight in 1970s; eighteen in the 1980s; and twenty six in the 1990s (UNDP, 2004).

Nepal falls on eleventh position on disaster venerability in the world and half of its population is under the risk of four types of disaster at a time including flood as mentioned the reported on Global Natural Disaster Risk Hotspots (Dilley et al., 2005). It is estimated that more than 1000 people die and around 40 thousand peoples get displaced with the devastating damage of infrastructure and economic resources of the nation by a number of disasters recurring every year; (ICHARM, 2008). While Nepal has unique geographical and climatic conditions with complex geology can explain the severity of water induced hazards, the vulnerability due to poverty, lack of public awareness, or inadequacy in preparedness, weak governance practices, little coordination among government and other agencies, inadequate financial resources, lower level of technical knowledge in mitigation of natural disaster.

The frequency and magnitude of floods seem to have increased in the last decades. Climatic changes, which are more noticeable all over the world, is often held responsible for changes in storms patterns and thus, increase in flood frequency. The other contributing factor is the constant spreading of urbanization areas over the rural lands, with the construction of concrete where soil once was, which contributes to increase the vulnerability of Floods are most common and widespread in Terai and Valley regions. The population growth of the country is increasing rapidly. The increased population needs more consumption. The people of the Terai encroaches the river bank and the hilly people influence to the forest resources. This trend has caused to poor managed to farming practice and that has caused the heavy landslide and soil erosion in hillside. Rivers carry the loads from the hill and deposit in Terai. This, the river spread is continuously increasing in Terai. In addition, the monsoon flood enters the settlement area, inviting the flood disaster in Terai.

The natural feature of flooding occurs when excess rainfall cannot be absorbed by the receiving soils or discharged fast enough by the stream network. In these conditions, the river sees its depth rising until the water can overtop its banks and spread throughout the adjacent flood plains. In areas where the river bed is surrounded by relatively flat lands, the flood plain can therefore be rapidly covered with a vast expanse of shallow water. After

the water retreats, flooding deposits silt on the flood plain and improves its fertility over decades. As a consequence, frequently flooded area used to attract agriculture and therefore human developments near the river, where soils are rich. Nowadays, human activities have changed, agriculture not at the centre of our society anymore, and flooding is now only seen as a natural disaster when water spreads throughout urban areas, where population and economic activities are usually concentred.

The rivers of Nepal can be classified into three categories:

1) Rivers originating from Himalayas and are perennial rivers; e.g. Koshi, Narayani, Karnali, and Mahakali. They originate from the Himalayas and after descending from the hills, flow through the Terai plains. During the monsoon (June-September), these rivers cause damage to the communities living within the floodplains.
2) Rivers originating from the Mahabharat range; e.g. Kankai, Kamala, Bagmati, West Rapti, and Babai. During monsoon, these rivers also cause a heavy damage in the communities living within flood plains in the Terai region.
3) Rivers originating from the Siwalik range; e.g. Ratu Khola, Lakhandehi Khola. These rivers have little flow during the dry season and some of them are almost dry. However, they are sometimes responsible for flash flooding during the wet season, causing heavy damage to the people living in the Terai plains.

1.2 CAUSES OF FLOOD IN NEPAL

Floods are common natural disaster phenomenon in Nepal. The factors triggering flood hazards in Nepal are: i) highly concentrated monsoon precipitation ii) high relief iii) steep mountain topography and iv) deep & narrow river valleys. Each year many people are killed and made homeless and property and infrastructure are damaged by floods. As a result, the overall development of the country has been severely affected by repeated flooding. In the future, the global warming phenomenon is likely to increase the frequency of flooding by increasing the intensity of extreme precipitation events and enhancing the melting of Glacier lake. The encroachment of areas susceptible to floods to establish human settlements and to carry out infrastructural development in the recent past has increased the exposure of these areas to flood hazards.

In Nepal, destroying floods are caused by different mechanisms which can be categorized into five major types:

a) Rainfall and cloudburst
b) Glacial lake outburst floods (GLOF)
c) Landslide dam outburst floods (LDOFs)
d) Floods induced by the failure of infrastructure
e) Sheet flooding or inundation in lowland areas

1.3 CURRENT STATUS OF FLOOD FORECASTING IN NEPAL

Flood forecasting is one of the major non-structural method to control the damages caused by flood. In Nepal there are no any operational flood forecasting system in Nepal. The current status of flood forecasting in Nepal is as follows.

- The Department of Hydrology and Meteorology (DHM), the only authorized collector and disseminator of hydro-meteorological data of Nepal, has established several hydrological and meteorological stations all over the country.
- Frequency of discharge measurement for developing rating curve is very low.
- High frequency discharge and rainfall data not available.
- Numerical weather forecast are not available
- There are only few telemetry systems to transmit data in real time which has been installed over end of 2010 and 2011 only.
- Data not available from Chinese part of trans-boundary River.
- Inadequate rain gauge network, no data on rainfall intensity and poor understanding of space and time variability of rainfall
- Full hydrological regime cannot be represented due to limited number of stream gauging stations
- No systematic snow measurement except a very few stations.
- Length of record is usually short.
- Continuous records of sediment load data are not available
- High-resolution of DEM are not available

- Although DHM has a unit named 'Flood Forecasting project', forecasting has not been started yet due to lack of real time data transmission system, forecasting model and dissemination system.
- Few trained hydrologists to produce reliable forecasts.
- Weak planning and preparedness for flood disaster mitigation
- Inadequate community awareness

1.4 STATEMENT OF THE PROBLEM

The main factors contributing to increased problem of floods in Terai can be classified as hydrological factor of high monsoon precipitation (natural cause) and human induced factor which includes human encroachment in the floodplain. Flood result from severe monsoon rainfall are the most significant natural disaster affecting Nepal in terms of their impact on the economic, damage to property and huge losses of life. So to aware the locality about the upcoming flood in the area flood warning can play a significant role.

In Nepal, like many other developing countries, the hydro-meteorological station networks are sparse and rainfall data are available only after a significant delay. According to the DHM of Nepal, the country average density is one gauge for about 331 km^2 and is especially very sparse in mountainous areas. Precipitation is highly variable in both space and time and is an important input in rainfall-runoff modelling.

Flood forecasting in basins with sparse rain gauges poses an additional challenge. Using hydrologic modelling techniques, it is possible to better prepare for and respond to flood events. Use of appropriate hydrologic models can mitigate flood damage and provide support to contingency planning and provide warning to people threatened by floods.

Structural methods of flood protection are neither economically viable nor these are environment friendly. There is a growing realization about the importance of non-structural measures including flood forecasting and early warning in flood management. It is important to make the flood early warning in the areas prone to flood hazards. Establishing a flood forecasting system would enhance the effectiveness of all other mitigation measures by providing time for appropriate actions. It may not be practical to

avoid floods but it is a worthy target to move toward minimal flood disaster damages from severity.

Flood early warning system in Nepal has not yet been carried out with proper planning and taking the problem into account at river basin scale. In view of increasing flood hazards one of the foremost need has been realized to equip a flood forecasting and warning system in River basins. The system can warn the inhabitants of flood plain corridor of the rivers so that they are aware of the forthcoming floods, especially during the year's monsoon periods.

This has increased the importance of flood modelling for flood forecasts to issue advance warning in severe storm situations to reduce loss of lives and property damage. But the accuracy of operational hydrological models primarily relies on good rainfall data input in terms of temporal and spatial resolution and accuracy (Pathirana et al.2005). For real time flood warning to be effective the rainfall information should also be made available real time, a capability though desirable but not available in most of the countries like Nepal. Recently, few stations are made real time by DHM.

1.5 NEED OF THE STUDY

The study of operational flood forecasting and warning system in Bagmati river basin provides an opportunity to estimate stream flow at the basin outlet for forecasting flood. As floods can neither be eliminated nor totally controlled so efforts are to be directed towards reducing flood vulnerability and mitigating the flood impact through improved flood managements. Hence a non-structural approach to flood management is useful in flood forecasting and early warning system. With an advance early warning system, a significant reduction in losses can be obtained by taking protective and preventive measures. The value of flood forecasting increases as the lead-time increases and hence effective and timely information dissemination to those responsible for disaster management and then directly to the people affected, would warn the local people about the upcoming flood and flooding time.

1.6 SCOPE OF THE STUDY

The scope of work includes the application of computer-based modelling tool like HEC-HMS and ArcGIS (with extension HEC-GeoHMS) that can provide effective and efficient

means of hydrological modelling. It includes pre-processing and spatial analysis of the Digital Elevation Model (DEM) for catchment delineation and stream network generation. It also includes the temporal data. The study aims at developing an event-based rainfall runoff model using HEC-HMS for the Bagmati River Basin, Nepal up to Bhorleni gauging site. Because of long expertise and experience in hydrological simulation, it is expected that the validated HEC-HMS model can be used to simulate flood events in the Bagmati River Basin for flood forecasting and related applications like deriving peak discharge and time of occurrence of the discharge for any rainfall in the basin. With the increase of the urbanisation and climate change the frequency of the flood has been increased in Bagmati River. Hydrological modelling helps in assessment of peak discharges based on terrain topography of the basin. With a view to this effect, the hydrological study of the basin is becoming more and more important to assess the peak discharge and the time of occurrence of such flood. The model would be useful for taking non-structural measures in the flood plain area.

1.7 OBJECTIVES

Flood forecasting and warning is an effective non-structural method of flood management by evacuating the affected persons along with their properties with the available of forecasted lead times. This method has been well expected by the planners and public in flood disaster mitigation and flood plain management. Recognizing this fact, DHM, Nepal is working for the development of flood forecasting and warning system in major rivers of Nepal. The general objective of the study is to extract the applicability of using modelling tools in Rainfall Runoff Modeling in Bagmati river basin of Nepal is the broader objective of this work. The specific objective of the study can be summarized as below.

1) To calibrate and validate HEC-HMS model for Bagmati River Basin at the Bhorleni Gauging outlet.
2) To formulate the real time flood forecasting using the calibrated and validated HEC-HMS model.
3) Updating real time flood forecasting using the error prediction model.

1.8 ORGANIZATION OF THE STUDY

This thesis has six chapters:

Chapter 1 contains an introduction, background information on flood, Causes of flood in Nepal, Current status of flood forecasting in Nepal, statement of the problem, need of the study, objective of the research, scope of study and organization of the study.

Chapter 2 presents review of literature and research gap

Chapter 3 provides the details of the study area and data availability

Chapter 4 includes methodology for flood modelling in HEC-HMS

Chapter 5 includes analysis and discussion of results

Chapter 6 presents the conclusions drawn from the study, limitation of the study and the scope for further study.

CHAPTER 2. LITERATURE REVIEW

2.1 REVIEW OF LITERATURE

Several studies have been carried out to understand the Real Time Flood Forecasting System. Under this section, some of the published research articles related to real time flood forecasting, are reviewed.

Baral M, (2008) carried the study on hydrological condition, basin scale rainfall runoff modeling and inundation analysis on Terai region of Nepal. To establish the relationship between rainfall and runoff to develop flood forecasting model, simple statistical tools for hydrological analysis and least square methods of best fit technique is applied within the available historical rainfall and stage data of the year 1980 to 2004. Flood frequency analysis is done and the floods of different return periods are identified. Inundation analysis is done based on available digital data, satellite images, and GIS based numerical models (Arc GIS, its extension HEC-GeoRAS and HEC-RAS software) together with some field observation data. The outcome of this study on finding the real time flood forecasting model and inundation depth for lower Bagmati watershed. The results of this analysis are understandable even to the community level people and such method can be applied to other river basins as well for non-structural counter measure of flood disaster mitigation.

Manoj et al. (2016) carried the study with the development of a flood forecasting model for Kielstau basin in Germany to analyze and estimate the runoff for developing flood control measures. The hydrology of the area is characterized by high interaction between ground water and surface water. Input files were prepared using HEC-GeoHMS and later imported to HEC-HMS along with the meteorological and hydrological data to calculate run-off at the watershed outlet. Analysis was carried out in HEC-HMS to determine peak stream flow and occurrence time. SCS-CN, Clark unit hydrograph, Muskingum and recession methods were used for loss, transformation, routing and base flow calculations respectively. The model was simulated for five sets of hourly rainfall values. The observed and simulated hydrographs showed high discrepancy due to poor rainfall-runoff data correlation and groundwater interaction. The model performance was evaluated using MAE (Mean Absolute Error) and RMSE (Root Mean Square Error).

Bras and Garrotte (1995) formulated a distributed model named as Distributed Basin Simulator (DBSIM) for the real-time rainfall-runoff simulation. It was based on extracting the topographical information made available by the Digital Elevation Models (DEM). When the storm proceeds through an area, the distributed rainfall data inputs are used to generate the maps of the evolving saturation areas. The runoff generation is estimated in grids by using kinematic infiltration model and relates the lateral inflow of moisture between the elements and surface flow routing in a simple way. Model calibration and verification was used to test the performance of the model.

Knebl et al. (2005) merged GIS and HEC-HMS to generate a regional scale flood model. The study was carried out using HEC-HMS software as a rainfall runoff model that transforms the precipitation excess to overland flow and channel discharge, as well as a hydraulic model in HEC-RAS that models the unsteady flow in the river network based on the hydrographs generated by the HEC-HMS The outcomes from this study can be used as an effective tool for developing flood predictions on a local or countrywide scale. It was initially designed for the San Antonio river basin but it can be applied to other basins also.

Huang et al. (2016) carried a study in real time flood forecasting system in Hsia-Yun watershed in Taiwan. The system incorporates four models: (1) a gray-based model to predict incoming rainfall intensities in the next 1–3 hour, (2) an antecedent hydrological condition estimation method to conclude time variant parameters before and during storms, (3) a computationally efficiency KW-GIUH model to perform runoff simulation, and (4) an updating algorithm to reduce forecasted runoff error.

Singh R.D. (2007) presented several real time flood forecasting models and procedures being used in India. In the formulation of real time flood forecast, the observed meteorological and hydrological data are transmitted to the forecasting station through different means of data communication which include telephone, wireless and network of telemetry stations etc. The structure of the model should be simple and it should not have unnecessary input requirements but at the same time the forecasted flood must be as exact as possible.

Halwatura et.al. (2013) collected rainfall, evaporation and other relevant data of five years. The rainfall-runoff transformation has been carried out using three different approaches; SCS curve number loss method, Snyder unit hydrograph method and Clark unit hydrograph method. The calibrated models are validated with new set of rainfall

runoff data, which showed that unit hydrograph method Clark and Snyder both were more reliable than SCS loss method.

Oloche & Zhi-Jhi (2010) carried out flood forecasting in Misai and Wan'an catchment in China; HEC-HMS Model has been used. The loss model adopted in the model was initial and constant loss method, rainfall runoff transformation method and SCS curve number transform method, base flow separation method was exponential recession method.

Choudhary et al. (2014) worked on the event-based simulation of rainfall runoff process in Balijore Nala watershed in Odisa, India, HEC-HMS model had been used with rainfall-runoff transformation method as SCS Curve number, Peak flow estimation as SCS unit hydrograph, base flow estimation as exponential recession, channel routing as Muskingum method. For the evaluation of the model, mean absolute relative error were used. During validation process, the performance of the model was found to be satisfactory.

The performance evaluation of conceptual (HEC-HMS) and spatial (ATHYS) model was done by Aquibat Ezziar, watershed Morocco (2014) on the basis of Nash Sutcliffe efficiency (NSE) and Rank sum ratio (RSR). Evaluation of the performance of the models showed that ATHYS had higher performance in estimation of peak flood **(Khattari et. al, 2016)**. The study reveals that continuous simulation with HEC-HMS model provides better performance.

Gautam, 2015 carried out his research work on effects of channel X-section in Gandaki River Basin, Nepal using HEC-HMS model. The simulation work was done on trapezoidal, rectangular and triangular channel section. The result of the study shows that using trapezoidal channel section is more efficient than triangular and rectangular section on the basis of Nash efficiency and degree of determination (R-squared value). The peak flow and time to peak at the outlet using trapezoidal channel section is nearly matched to the observed peak flow and time to peak for calibration and verification period than other sections. However the average annual flow and total annual volume at the outlet is nearly same using trapezoidal and triangular sections and to some extent deviated from observed mean flow and annual volume respectively. Based on the outcome of this study, the trapezoidal channel section is most suitable for flood forecasting with continuous simulation.

Kar and Lohani (2010) considered on advancement of Flood Forecasting System Using Statistical and ANN Techniques in the Downstream Catchment of Mahanadi Basin, India. Fist Statistic approach was used and later ANN technique was applied for downstream Hirakud catchment between stations Khairmal, Barmul and Mundali. The estimating gained by both the procedures was inspirable. ANN technique had a superior output in comparison to statistical technique. The statistical technique can also give satisfactory result. The optimum result for travel time assessment of Khairmal-Mundali reach was efficiency is 80.11% and RMSE is 2.55. As the information recording is of 3-hour interval this sort of result was still encouraging. The travel duration used between base station and forecasting stations differs nearly 24-37 hour.

Xiong L. and Connor K.M.O (2002) carried and investigated out on study of four different updating models: single autoregressive (AR) model, autoregressive-threshold (AR-TS), fuzzy autoregressive-threshold (FU-AR-TS) and artificial neural network (ANN) model. The lumped soil moisture accounting and routing (SMAR) conceptual model had been selected to simulate the observed discharge series on 11 selected test catchments in the application of these four updating models. . It is found that all of these four updating models are very successful in improving the flow forecast accuracy, when operating in real-time forecasting mode. Past experiences have shown that in real-time flow forecasting, single autoregressive (AR) model is very efficient in simulating the forecast errors from the fundamental model operating in the simulation (i.e. non updating) mode (WMO, 1992). The authors inspected whether such latest mathematical tools, as fuzzy system and artificial neural network (ANN) models, now widely used in hydrology, can produce more efficient updating schemes than the single AR updating model.

2.2 RESEARCH GAP/ RATIONAL

Nepal is considered a disaster-prone country throughout the world. Flooding is one of the major natural hazard causing damages worth millions of dollars every year. There is developing acknowledgement about the significance of non-structural measures including flood forecasting and early warning in flood management. Establishing the flood forecasting system upgrades the viability of all other relief measures by giving time to proper activity. This has expanded the significance of flood modelling for flood forecast to issue guidance in severe storm to diminish life and property harm. Few research works have been carried out in this basin regarding rainfall runoff modelling. In the past research

work conducted in the Bagmati River Basin; daily rainfall data and the corresponding maximum instantaneous discharge were used to predict flood hydrograph. One of the limitations of that study was that it was not able to predict time of occurrence of peak flood accurately. Using hourly data eliminates this drawback in this research work. The Department of Hydrology and Meteorology, Nepal is working for the development of flood forecasting and warning system for Bagmati River Basin. Even though a number of flood forecasting studies were carried out in the Bagmati River Basin over the decades, their results have not been implemented so far. From the literature review carried out, it is observed no scientific study of real time flood forecasting using HEC-HMS model has yet been attempted for this Bagmati River Basin.

CHAPTER 3. DESCRIPTION OF STUDY AREA AND DATA AVALABILITY

3.1 STUDY AREA

The Bagmati river is one of the important river basin of Nepal with monsoon rain and springs as main sources. The Bagmati River basin originates from the Shivapuri hills of the Mahabharata range and drains out of Nepal (Jha 2002) across the Indian State of Bihar to reach the Ganges. Its total length is 597 km of which 206.8 km lies in Nepal (DWIDP, 2005). Its main tributaries –Manohara, Bishnumati, Kulekhani, Kokhajor, Marin, Chandi, Jhanjh and Manusmara and is situated within the middle mountain of Nepal (26º42'-27º50' N —85º02'-85º58' E) having an area of 3,750 km2. Babel et al. (2013) has mentioned that the elevation of the Bagmati River basin ranges from 80 m in Terai in the southern part of Nepal to 2900 m in the Mahabharata range in the north. Here for study analysis the Bagmati river Basin upto the Bhorleni gauging site is taken which lies about 38 kilometers upstream of Pandheradovan gauging station. The catchment having area 1694.31 sq.km is partially covered with Kavre and Makwanpur districts and fully covered with Kathmandu, Lalitpur, Bhaktapur districts. The location map of the Bagmati River Basin up to Bhorleni gauge station is presented in Figure 3.1.

Every year in monsoon season, high flood at Bagmati River is causing loss of lives and property in the downstream reach of the basin. Due to increasing trend of extreme events and present economic condition of the country, government will not be able to afford huge structural interventions for the entire watershed. Thus, combination of structural as well as community approach of non-structural flood disaster management would be most economical and effective method of flood disaster mitigation to save the life and property in the Terai region of Bagmati river basin. Department of Hydrology and Meteorology (DHM) has established more than twenty climatological stations within and in the nearby of the catchment area and five discharge gauging stations in the Bagmati River Basin. Among all climatological stations, Daman and Manusmara are the highest and lowest altitude stations with elevations of 2314 m and 100 m respectively. Sundarijal (Station No.505) and Pandhera Dobhan (Station No.589) are the highest and lowest altitude discharge gauging stations with elevations of 1600 m and 180 m respectively.

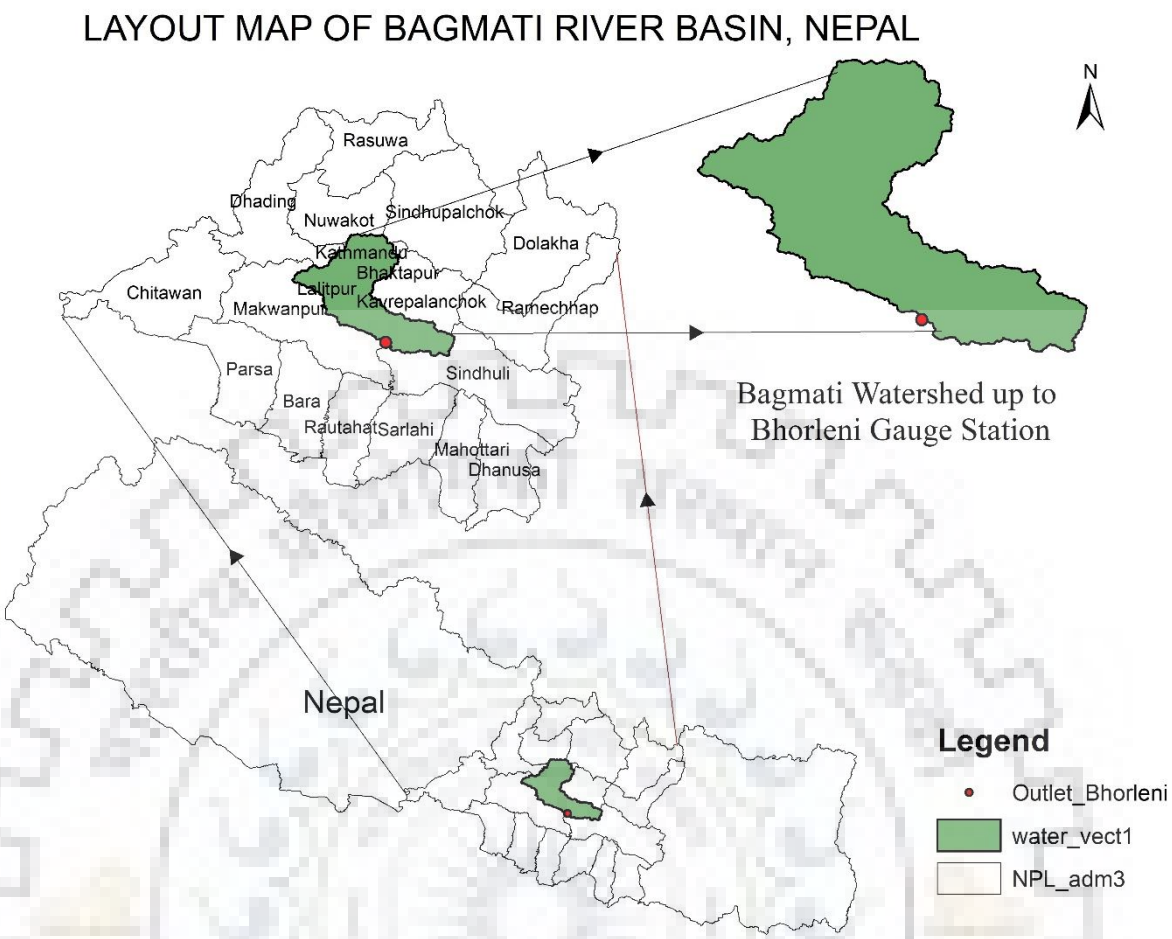

Figure 3.1 Location Map of Study Area

3.2 DATA AVAILABILITY

3.2.1 METEOROLOGICAL AND HYDROLOGICAL DATA

In the present dissertation work, hourly data of precipitation, gauge and discharge and as well as daily data of precipitation, gauge and discharge are selected for extreme flood events. Eleven meteorological stations; Budhanilkantha (Station no.1071), Chisapani Gadi (Station no.904), Godavari (Station no.1022), Hariharpur Gadi (station no.1117), Kathmandu Airport (Station no.1030), Khokana (Station No.1073), Lele (Station no.1075), Nagarkot (Station no.1043), Nepalthok (Station no.1001) Sundarijal (Station no.1074) and Thankot (Station no.1015), and only one discharge station; Bhorleni (Station no.581) are selected for analysis due to availability of data. These data were collected from the Department of Hydrology and Meteorology, Nepal for model calibration and validation. The selected flood events are shown in Table 3.1.

Table 3.1 Meteorological and Hydrological Data

S.N	Rainfall Station	No. of Events	Selected Flood events
1	Budhanilkantha	3	2 July 2018 03:00- 4 July 2018 02:00 12Aug 2018 16:00 - 14 Aug 2018 17:00 11 July 2018 19:00 - 14 July 2018 00:00
2	Chisapani Gadi	3	2 July 2018 03:00- 4 July 2018 02:00 12Aug 2018 16:00 - 14 Aug 2018 17:00 11 July 2018 19:00 - 14 July 2018 00:00
3	Godavari	3	2 July 2018 03:00- 4 July 2018 02:00 12Aug 2018 16:00 - 14 Aug 2018 17:00 11 July 2018 19:00 - 14 July 2018 00:00
4	Hariharpur Gadi	3	2 July 2018 03:00- 4 July 2018 02:00 12Aug 2018 16:00 - 14 Aug 2018 17:00 11 July 2018 19:00 - 14 July 2018 00:00
5	Kathmandu Airport	3	2 July 2018 03:00- 4 July 2018 02:00 12Aug 2018 16:00 - 14 Aug 2018 17:00 11 July 2018 19:00 - 14 July 2018 00:00
6	Khokana	3	2 July 2018 03:00- 4 July 2018 02:00 12Aug 2018 16:00 - 14 Aug 2018 17:00 11 July 2018 19:00 - 14 July 2018 00:00
7	Lele	3	2 July 2018 03:00- 4 July 2018 02:00 12Aug 2018 16:00 - 14 Aug 2018 17:00 11 July 2018 19:00 - 14 July 2018 00:00
8	Nagarkot	3	2 July 2018 03:00- 4 July 2018 02:00 12Aug 2018 16:00 - 14 Aug 2018 17:00 11 July 2018 19:00 - 14 July 2018 00:00
9	Nepalthok	3	2 July 2018 03:00- 4 July 2018 02:00 12Aug 2018 16:00 - 14 Aug 2018 17:00 11 July 2018 19:00 - 14 July 2018 00:00
10	Sundarijal	3	2 July 2018 03:00- 4 July 2018 02:00 12Aug 2018 16:00 - 14 Aug 2018 17:00 11 July 2018 19:00 - 14 July 2018 00:00
11	Thankot	3	2 July 2018 03:00- 4 July 2018 02:00 12Aug 2018 16:00 - 14 Aug 2018 17:00 11 July 2018 19:00 - 14 July 2018 00:00
S.N	**Hydrological Station**	**No. of year**	**Discharge for Selected Flood Events**

1	Bhorleni	1	July 2018, August 2018

3.2.2 SPATIAL DATA

The Digital Elevation model (DEM) and Satellite Image of 30m resolution which is freely available were downloaded from United States Geological Survey (USGS) website. The DEM is the fundamental need of the HEC-Geo HMS tool to create the basin model of this study area. And the source of land use land cover data map was downloaded from International Centre for Integrated Mountain Development (ICIMOD).

CHAPTER 4. METHODLOGY

4.1 SPATIAL DATA PROCESSING

4.1.1 PREPARATION OF BASIN MAP AND DELINEATION OF DRAINAGE NETWORK

The basin map for Bagmati river up to Bhorleni gauging site was prepared using the SRTM raw DEM data downloaded from USGS website using ARCGIS software and also the drainage stream network of the river basin was delineated using the same software. The tool namely "hydrology", available in ARCGIS toolbox was used to define the river basin.

4.1.2 PREPARATION OF DIGITAL ELEVATION MODEL

The raw DEM and shape file of the delineated basin were used to prepare final DEM considering the different elevation classes and the terrain surface of the basin was identified.

4.1.3 PREPARATION OF THIESSEN POLYGON MAP AND COMPUTATIONS OF THIESSEN POLYGON WEIGHTS

The Thiessen polygon map was prepared using the tool "Thiessen Polygon", available in ArcGIS software. The geographical coordinates of each rainfall stations were supplied as input to the software. The gauge weights were computed using the ArcGIS software. The computed gauge weights were considered as input to the HEC-HMS under its Meteorological Model.

4.1.4 PREPARATION OF LAND USE / LAND COVER MAP (LULC)

The LULC map was prepared using the "clip" tool of ArcGIS for extracting the LULC map of the basin from International Centre for Integrated Mountain Development (ICIMOD) (http:/rds.icimod.org) where such maps are available in digital form.

4.1.5 PREPARATION OF ISOCHRONAL MAPS AND DEVELOPMENT OF TIME AREA CURVE

An isochrone is a line on the catchment map joining points having equal time of travel of surface runoff. For preparing the isochronal map of the basin, some points located on the

Bagmati River and its tributaries in the basin were identified using HEC-GeoHMS. The time of travels from all these points up to Bhorleni Gauging site were required to be estimated. In this regard, the time of travels of all the segments obtained from considering the two consecutive points on the streams, were taken to be directly proportional to$L\sqrt{S}$. This can be demonstrated from the Manning's equation which is as follows:

$$\boldsymbol{V = \frac{R^{2}/_{3}\, x\, S^{1}/_{2}}{n}} \quad (4.1)$$

Where ***V*** is average velocity of the stream in m/s at the end of the segment,

R is hydraulic radius in m for the stream cross section at the end of the segment,

S is average longitudinal slope of the channel segment and

n is Manning's Roughness Coefficient of the channel segment at its end

However, the Manning's equation can be rearranged in terms of stream length L and time of travel t_c considering the end channel as a wide rectangular channel and $V=L/t_c$. The equation may be written as:

$$\boldsymbol{t_c = C.\ L/\sqrt{S}} \quad (4.2)$$

Where $\mathbf{C=R^{2/3}/n}$. It is considered to be constant.

The time of travel from the farthest point of the catchment to the outlet of the basin along the longest stream was considered as time of concentration of the catchment (T_c). The time of travel for ith segment was computed as $t_{ci}=C.\ L/\sqrt{Si}$. Subsequently, the time of travel for each river was computed as the C times sum of the $L/\sqrt{S}$ for each individual segments of the river and the tributaries i.e [C $(L1/\sqrt{S}1 + L2/\sqrt{S}2 + L3/\sqrt{S}3 \ldots\ldots + L/\sqrt{S}n)$], where n is number of segments for any river reach. The maximum value of $C\sum(\frac{L}{\sqrt{S}})$ was found from all the river reaches. It was equal to time of concentration (T_c). Thus

$$T_c = C\sum(L\ /\ \sqrt{S}) \quad (4.3)$$

An initial estimate of T_c was obtained from the excess rainfall hyetograph and direct surface runoff hydrograph for a storm event. The T_c is the time from the end of excess rainfall to point of inflection on the recession limb of the direct surface runoff. Now the

equation (4.3) was used to get the value of constant C knowing the value T_c and $\sum(L / \sqrt{S})$ for the longest flow path.

Here, the Time-Area curve was developed using the Inverse Distance Weighted (IDW) method. It was presented in the form of Times-Area Histogram as well as cumulative Time-Area Percent curves which was the input in HEC-HMS under Clark transform model in "Paired Data".

4.2 TEMPORAL DATA PROCESSING

4.2.1 RAINFALL DATA PROCESSING

Eleven rain gauge stations were selected on the Bagmati River basin up to Bhorleni Gauging site. Out of the eleven stations five stations are the hourly rainfall values and the remaining six stations are the daily rainfall values. The daily rainfall values are then converted into hourly values taking nearest SRRG (Self Recording Rain Gauge) stations. For each storm events, the average hourly rainfall values for the basin were computed using the gauge weights obtained from the Thiessen Polygon method.

4.2.2 STREAM FLOW DATA PROCESSING

The stream flow data i.e. measured discharge is key for adjustment and approval of the formulated model in HEC-HMS which is required for calibration and validation purposes. Only one discharge gauge station- Bhorleni was selected due to availability of data. There was no hourly stream flow data at the gauging site of the outlet considered. From the observed daily gauge and discharge data, stage-discharge relationship which is also known as Rating Curve for the gauging site was established. It shows the relationship between average discharges with stage at particular location. If G indicates stage for discharge Q, then the relationship between G and Q can be explained with the equation:

$$\boldsymbol{Q = Cr(G - \alpha)^{\beta}}$$

Where Cr and β are the empirical constants or rating constants

The hourly discharge values were calculated at the gauging site of the outlet using the developed rating curve corresponding to hourly observed stages.

4.3 APPLICATION OF HEC-GEOHMS AND HEC-HMS

The Geospatial Hydrologic Modeling System (HEC-GeoHMS) is an extension to ArcView GIS. GeoHMS uses ArcView and Spatial Analyst to develop a number of hydrologic modelling inputs i.e. to develop basin model and its characteristics from the raw digital elevation model (DEM) in the convenient manner. Here, basin model is created by HEC-GeoHMS with a single basin and used for calibration and verification process. The required basin characteristics such as longest flow path, river lengths, upstream and downstream elevations and slopes of each river segments are obtained through this HEC-GeoHMS application process. Analysing digital terrain information, HEC-GeoHMS transforms the drainage paths and watershed boundaries into a hydrologic data structure that represents the watershed response to precipitation. In addition to the hydrologic data structure, it includes the development of grid-based data, physical watershed, stream characteristics and background map file for model in linear semi-distributed runoff transformation, the HEC-HMS basin model. The program features has terrain pre-processing capabilities in both interactive and batch modes. Additional interactive capabilities allow users to construct a hydrologic schematic of the watershed at stream gages, hydraulic structures, and other control points. The element network of the basin which was represented in HEC-HMS desktop was also performed by HEC-GeoHMS. Then the developed basin model representing element network in HEC-GeoHMS is imported to Hydrologic Modeling System, HEC-HMS for its further application. HEC-HMS is the simulation software developed to simulate all type of hydrological process of watershed. It is a freeware and can be downloaded on the official website of HEC4.2.1. The entire modelling process mainly is executed by the software namely HEC-GeoHMS and HEC-HMS. Figure 4.1 illustrates the calibration and validation process of the modelling of this study.

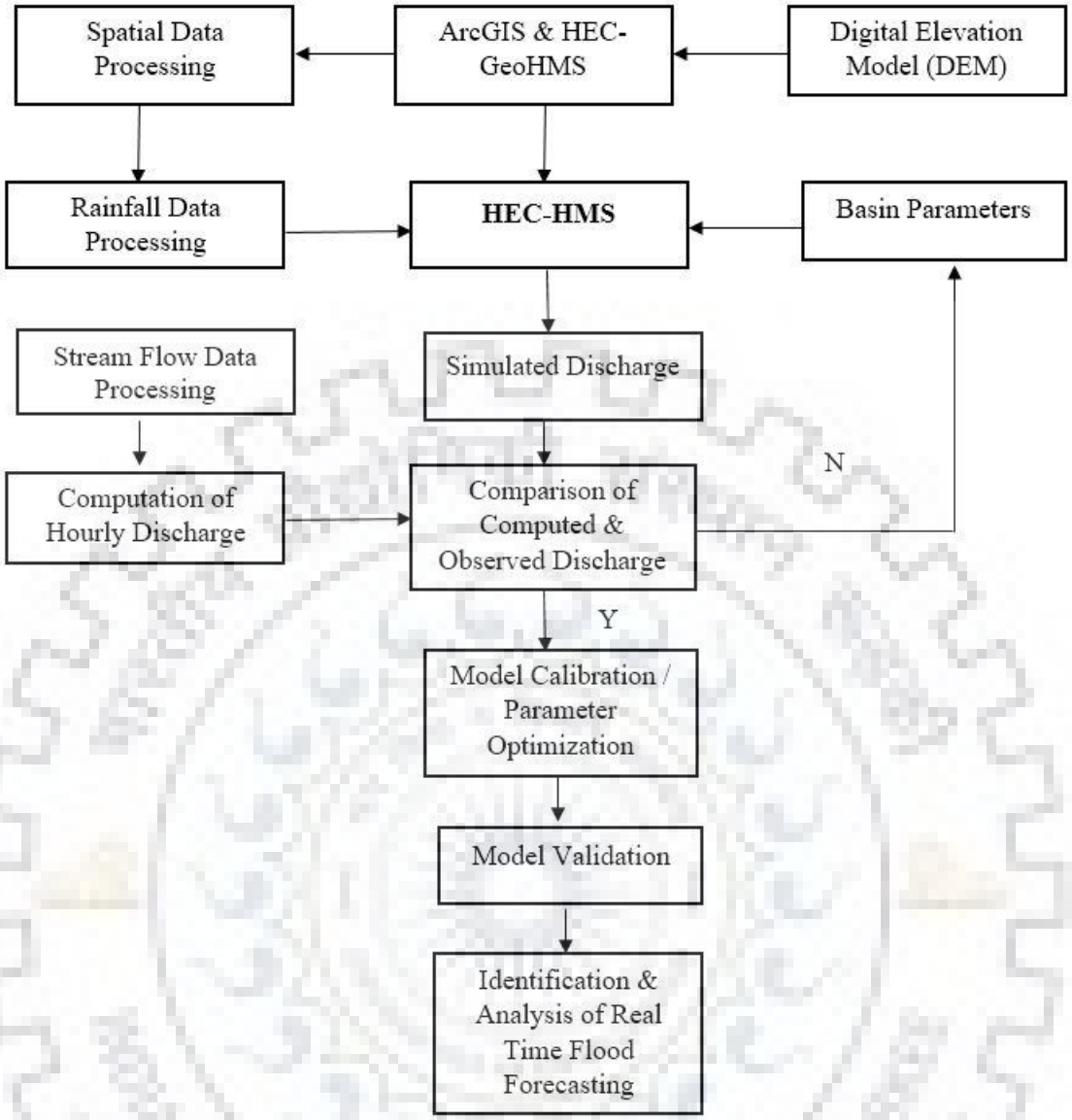

Figure 4.1 Flow Diagram of HEC-HMS Process

4.3.1 METEOROLOGICAL MODEL

Atmospheric condition over the catchment area and land surface can be represented by meteorological model. During preparation of meteorological model, the main purpose is creating meteorological boundary condition in the catchment area under study. It includes user specified hyetograph, gauge weighted average, thiessen method and inverse distance methods. Here for the study, meteorological model is created by selecting gage weights option available in the HEC-HMS model. Gage weights, which have been estimated from Thiessen polygon method, are used for this option.

4.3.2 BASE FLOW MODEL

There are three options available in the HCE-HMS program for the computation of base flow. They are:

a) Constant, Monthly- varying value
b) Exponential recession model
c) Linear – reservoir accounting model

In this study, the exponential – recession model was used for separating the base flow from the flood hydrographs resulting due to different storm events in order to estimate the direct surface runoff hydrographs. This base flow model, which defines the exponential form of relationship is described as

$$Q_t = Q_o K^t$$

Where, Q_t = the base flow in m^3/s (at any time), Q_o is the initial base flow in m^3/s (at time zero) and k is an exponential decay constant or recession constant.

In base flow model, the contribution of base flow decays exponentially from the initial flow. As per the HEC-HMS program, *k* is defined as the ratio of the base flow at time *t* to the base flow one day earlier. The base flow model includes the parameters such as initial base flow, the recession constant and the threshold flow.

4.3.3 LOSS MODEL

There are numerous runoff volume models also known as loss models are applicable in HEC-HMS modeling.

i) Initial and Constant Rate Loss Model
ii) Deficit and Constant Rate Loss Model
iii) SCS-CN Loss Model
iv) Green and Ampt Loss Model
v) SMA Loss Model

For this study area, in the application of loss model, the method Initial loss and Constant rate is used. This method includes two parameters such as initial loss (I_a) and constant loss rate. These parameters are highly depending on the physical properties of the river basin, land use and the antecedent moisture condition.

4.3.4 TRANSFORM MODEL

There are various transform models in HEC-HMS program which are as given below

i) Clark UH Model
ii) SCS UH Model
iii) Snyder UH Model
iv) Mod. Clark Model
v) Kinematic Wave Model

In this study, the Clark UH model and Snyder UH transform models were used for the event-based rainfall-runoff modeling.

4.3.4.1 CLARK UH MODEL

It is a synthetic unit hydrograph developed by Clark (1945). He has considered the effects of translation and attenuation for the generation of flow in the catchment area. The basic concept of this model defines that the temporary storage of water over the basin (in the soil and channels) plays important role in the transformation of rainfall excess to direct runoff. The linear reservoir relationship is generally used to show the effects of this temporary storage. The linear reservoir relationship may be represented with the following continuity equation.

$$\frac{dS}{dt} = I_t - O_t \tag{4.11}$$

Where *dS/dt* is the time rate of change of water in storage at time t; I_t is the average inflow to the storage at time *t*; and O_t is the outflow from storage at time *t*.

Storage and outflow at time *t* have the relationship with the linear reservoir model as follows.

$$S_t = R.O_t \tag{4.12}$$

Where R is constant linear reservoir parameter (storage coefficient). From the above equations (4.1) and (4.12), the following relationships are obtained.

$$O_t = C_A I_t + C_B O_{t-1} \tag{4.13}$$

Where C_A and C_B are routing coefficients. The computation of these coefficients are given below:

$$C_A = \frac{\Delta t}{R+0.5\Delta t} \tag{4.14}$$

$$C_B = 1 - C_A \tag{4.15}$$

The average outflow is given by

$$\overline{Ot} = \frac{Ot + O_{t-1}}{2} \tag{4.16}$$

Since the cumulative effects of all basin storage is represented in this Clark UH model, the reservoir may be considered to be located conceptually at the outlet considered. In addition to this lumped model of storage, the Clark UH model computes the time required for water to move outlet from basin. It carries out with linear channel model in which water is routed from remote points to the outlet with delay (translation) but without attenuation. This delay is implicitly related with time and area so called time area histogram. This specifies the basin area contributing flow at the outlet as a function of time. If the area is multiplied by the unit depth of excess rainfall and divided by the time step Δt, the result is inflow, I_t, to the outlet (linear reservoir)

Application of Clark transform model in HEC-HMS requires the following parameters:

a) Time of Concentration, T_c
b) The Storage Coefficient, R
c) The properties of Time-Area histogram or Time-Area Percent Curve of the basin

The time of concentration T_c and the storage coefficients R were estimated from sensitive analysis to employ as initial parameter values. The time-area percent curve is developed using Inverse Distance Weighted (IDW) Interpolation method.

4.3.4.2 SNYDER UH MODEL

In the Snyder UH model, the critical characteristics of the UH are the lag, peak flow and total time basin. Snyder (1938) stated the following relationship for a standard UH.

$$t_p = 5.5t_r \tag{4.17}$$

Where t_r is the rainfall duration, t_p is the basin lag which means the difference time of UH peak and the time of centroid of the excess rainfall of hyetograph. If the desired UH for a specific basin is significantly varied from standard UH, the following relationship may be defined to compute the lag of desired UH.

$$t_{pR} = t_p - \frac{t_r - t_R}{4} \tag{4.18}$$

Where t_R is duration desired UH and t_{pR} is lag of desired UH. Snyder further found that the following relationship in the case of standard UH.

$$\frac{U_p}{A} = C\frac{C_p}{t_{pR}} \tag{4.19}$$

Where U_p is peak of standard UH, A is basin drainage area, C_p is UH peaking coefficient and C is conversion constant (2.75 for SI unit). For other desired UH, the UH peak U_{pR} is defined as:

$$\frac{U_{pR}}{A} = C\frac{C_p}{t_{pR}} \tag{4.20}$$

Snyder model in HEC-HMS requires two parameters:

a) Standard lag, t_p
b) Peaking Coefficient, C_p

The HEC-HMS programme uses the computed UH peak and time to peak to find an equivalent Clark's model UH. From this approach, it computes the time base and all ordinates except the peak of UH. However, the initial values for the Snyder UH model were obtained from the result of sensitivity analysis.

4.4 SENSITIVITY ANALYSIS

A sensitivity analysis is usually undertaken in most modeling studies. It is necessary process to identify the key parameters and parameter precision required for calibration. Here for the study; the sensitivity analysis was carried out for two transform models: Clark and Snyder models in order to define the range of initial parameters to be considered during the optimization. In this regard, NSE values were computed for different sets of parameters values for Clark and Snyder models. As the Clark UH and Snyder UH models are two parameters models, NSE contours were drawn considering different values of one parameter on x-axis and correspondingly the other parameter values on y-axis. Such contours were helpful for identifying the band of the maximum NSE value. Finally, the

initial parameters values of those transform models were decided considering them within this band.

4.5 Error Criteria For Comparing the Performance Of Two Transform Models

For comparing the performance of the two transform models; Clark and Snyder models during calibration and validation, the following error criteria were obtained through HEC-HMS software based on the observed and computed direct surface runoff hydrographs.

a) Nash-Sutcliffe Model Efficiency (NSE)

The efficiency for evaluating the performance of hydrological models as proposed by Nash and Sutcliffe (1970) has been defined by the following relation.

$$NSE = 1 - \left[\frac{\sum_{i=0}^{n}(Qobs(i)-Qcom(i))^2}{\sum_{i=0}^{n}(Qobs(i)-Q)^2}\right] \quad (4.21)$$

Where $Qobs$, $Qcom$ and Q are the observed, simulated and observed mean discharge over the *n* hours respectively. The most optimal value of NSR is 1.

b) Volume Deviation (*Dv*)

This method of evaluation of model only considers the quantity of simulated volume but does not consider the peak volume and its timings. The percentage error in volume deviation was computed using the equation:

$$Dv = \left|\frac{(Vobs-Vcom)}{Vobs}\right| x\ 100\% \quad (4.22)$$

Where $Vobs$ and $Vcom$ are the observed and simulated volume of runoff over the *n* hours respectively. The most optimal value of *Dv* is 0.

c) Percent error in Peak (*Z*)

This method of evaluation considers the magnitude of peak flow only. It does not take into account of calculated volume and time of peak. The percent error in peak flow can be determined by the following relation:

$$Z = \left|\frac{Qobs(peak)-Qcom(peak)}{Qobs(peak)}\right| x\ 100\% \quad (4.23)$$

Where $Qobs(peak)$ and $Qcom(peak)$ are the observed and simulated peak discharge of runoff over the n hours respectively. The most optimal value of *Z* is 0.

The *NSE* was reported as best performance criteria of simulation (Mc Cuen et al.2006). However, in addition to the *NSE*, percent error in peak, percent error in time to peak, percent error in discharge volume of each direct runoff model were compared individually for each of the flood events considered for calibration and validation.

4.6 CALIBRATION AND VALIDATION

Transform models were calibrated using the automatic calibration i.e. optimization option available in HEC-HMS. While taking the optimization runs, the initial parameter values of the models were required to be estimated. In this regard, sensitive analysis was carried out for estimating the parameters. The calibrations of the model were carried based on the various goodness of fit measures derived from the observed and simulated hydrographs in HEC-HMS programme. Based on these measures, the optimized parameters of the transform models were selected. Calibration was carried out for selected number of events and the representative parameters were derived taking the average of the optimized parameters obtained for each event considered for calibration. The representative parameters of two transform models: Clark and Snyder models were used in HEC-HMS for their validation over the selected storm events not considered for calibration.

4.7 REAL TIME FLOOD FORECASTING

Of all the non-structural measures, flood forecasting and warning is the most widely accepted and has been used since the latter half of the 20th century. It supplements almost all other structural as well as non-structural measures. Flood forecasting involves estimating when a flood is likely to cause damage or loss of life, what its magnitude will be (usually in terms of its maximum stage at a given location) and how long it will last. Flood forecasting may be defined as "the process of estimating the future stages or flows and its time sequence at selected points along the river during floods". Flood forecasts refer to prediction of "the crest and its time of occurrence" and logical extension to the stages of river above a specified water level called the "Warning Level". Thus, the forecasts are made based on the current condition called real time forecasting and time (interval) over which a forecast is made called lead time.

Efficient water resources planning and management requires continuous forecast of river discharge over a given period. Such forecast would be helpful in operating the component of water resources systems to avoid or reduce the flooding in downstream areas to the extent possible and to issue warning to evacuate the flood prone areas along the reach. The flooding is normally due to high intensity of rainfall in the catchment. The development of flood forecasting is essential to manage such hazards. Here, the goal is to obtain real time precipitation and stream flow data through a microwave, radio or satellite communications and insert the data into rainfall-runoff and stream flow routing programs and forecast flood flow rates and water levels for periods varying from a few hours to a few days ahead, depending on the size of watershed. A further important factor is whether or not rainfall and flow data are available in real time. If so, flood forecasts can be updated at each time point a new data become available.

4.7.1 DEVELOPMENT OF UNIT HYDROGRAPH

The unit hydrograph was developed using the validated parameters of the best transform model using the HEC-HMS.

4.7.2 FORECASTING OF FLOOD HYDROGRAPH

The direct surface runoff hydrograph was forecasted at hourly time step considering the information available for excess rainfall till that time step using the principle of proportionality and principle of superimposition inherent with the unit hydrograph.

4.8 UPDATING REAL TIME FLOOD FORECASTING

For this research work, error prediction of real time flood forecasting has been updated using the method of multiple linear regression. The simulation error (residual error) of the rainfall-runoff errors are obtained as

$$E = E_o - E_s \tag{4.81}$$

Where E is the residual error

E_o= ordinates of Observed Hydrograph

E_s= corresponding ordinates of Simulated Hydrograph

Now, model of the Error $E_i$can be determined as in the form of equation below:

$$E_i = a_1E_{i-1} + a_2E_{i-2} + a_3E_{i-3} + \cdots \ldots\ldots\ldots\ldots\ldots + a_nE_{i-n} + Constant \tag{4.82}$$

Where i is the number of hours taken to update the simulated forecast hydrograph,

$a_1, a_2, a_3 \ldots . \ a_n$ are the coefficients obtained from the multiple linear regression method.

Thus, the updated forecast can be obtained by adding the values of model of Error, E_i with the values of simulated hydrograph, E_s.

CHAPTER 5. ANALYSIS AND DISCUSSION OF RESULT

5.1 SPATIAL DATA PROCESSING

5.1.1 PREPARATION OF BASIN MAP AND DELINEATION OF DRAINAGE STREAM NETWORK

Figure 5.1 shows the basin map for Bagmati River up to Bhorleni gauging site was prepared using the SRTM raw DEM data downloaded from USGS website using ARCGIS software and also the drainage stream network of the river basin was delineated using the same software. The tool namely "hydrology", available in ARCGIS toolbox was used to define the river basin. The shape of the river basin seems to be significantly irregular shape.

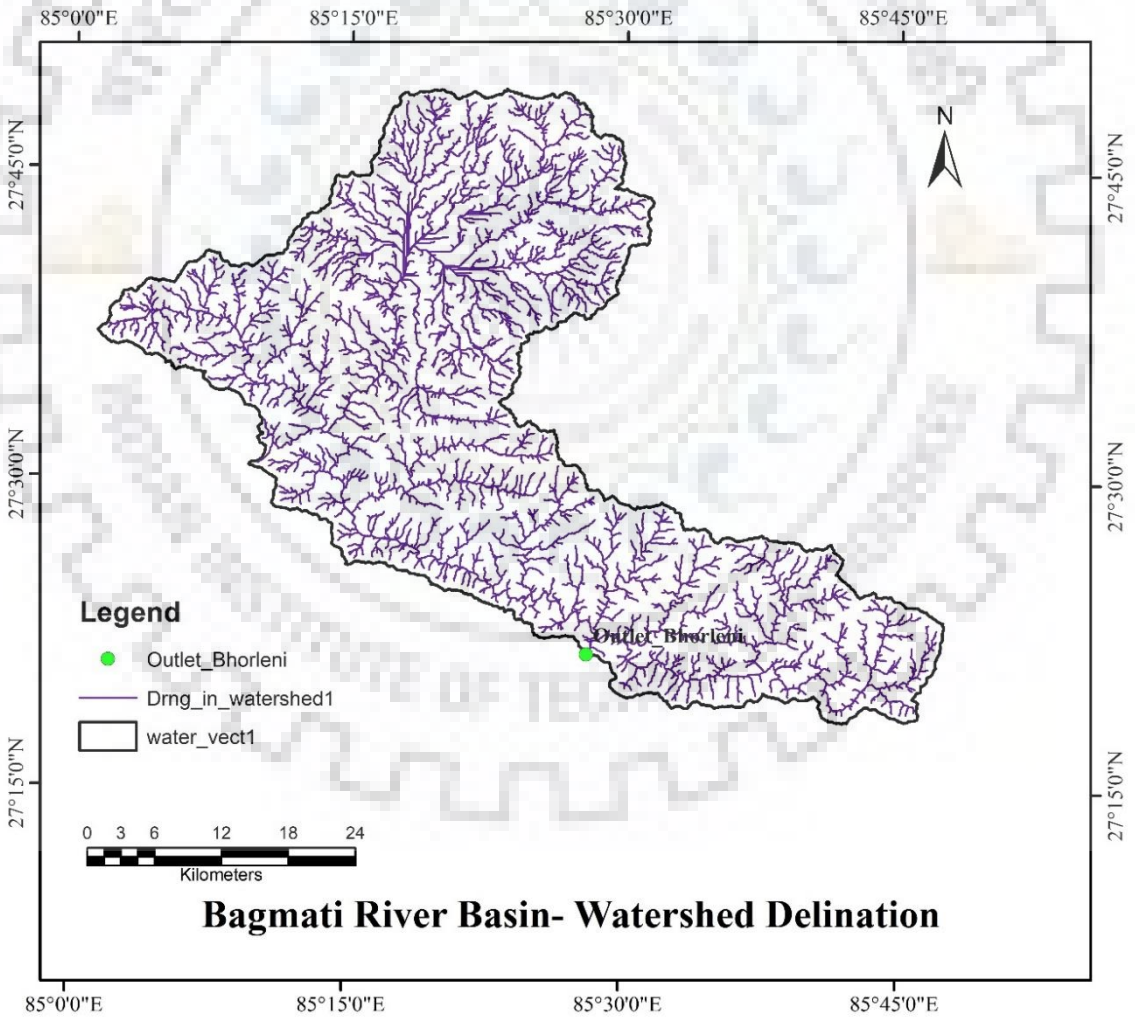

Figure 5.1 Delineated Watershed & Drainage Network of Bagmati River Basin up to Bhorleni Gauging Site

5.1.2 PREPARATION OF DIGITAL ELEVATION MODEL

The digital elevation model was used to prepare digital elevation map of Bagmati River Basin up to Bhorleni gauging site. Figure 5.2 shows the digital elevation map of the Bagmati River basin. The major portion of the river basin is hilly having elevation range varying between 261m to 2921 m above MSL.

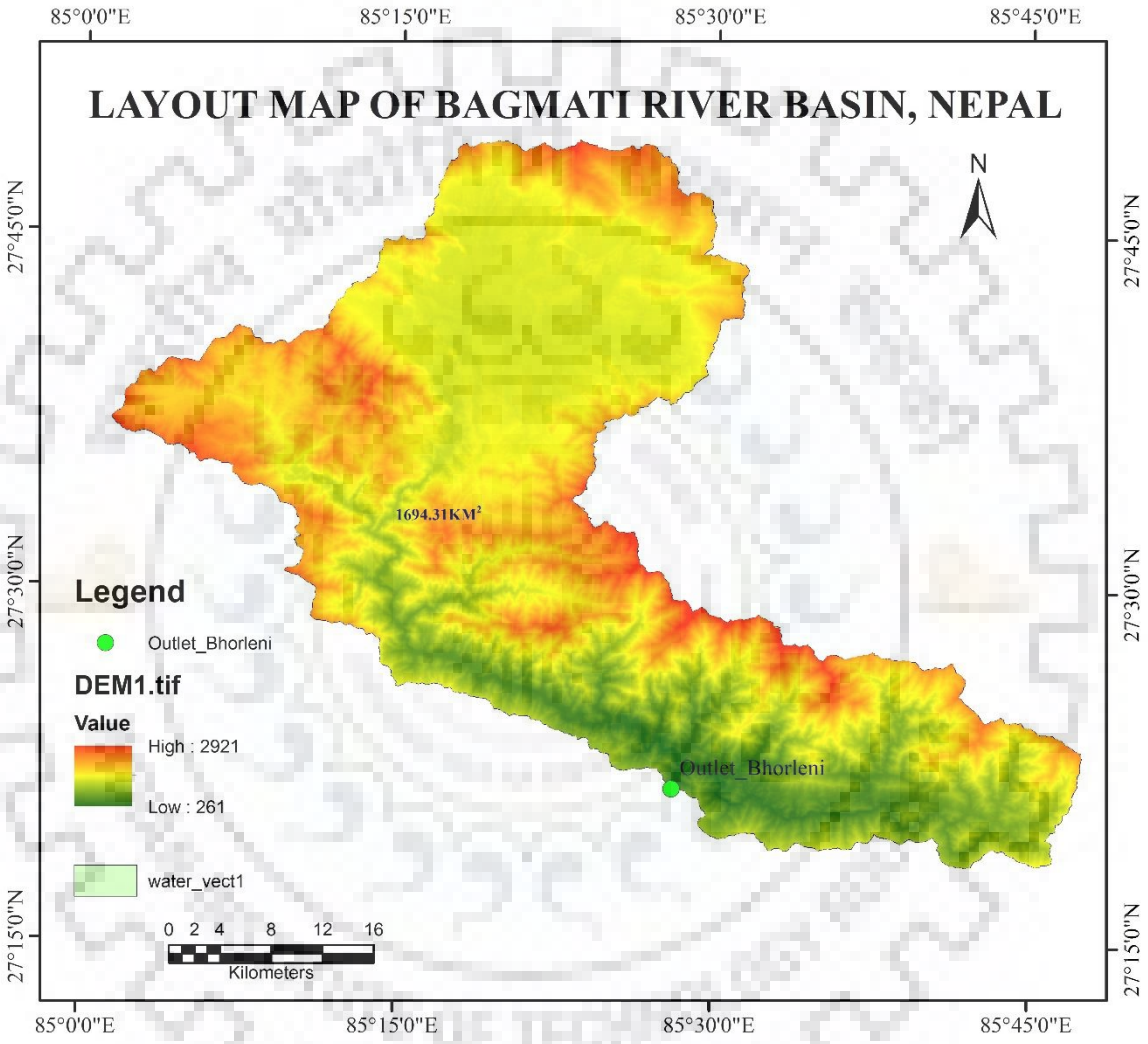

Figure 5.2 Digital Elevation Map of Bagmati River Basin up to Bhorleni Gauging Site

5.1.3 PREPARATION OF THIESSEN POLYGON MAP AND COMPUTATIONS OF THIESSEN POLYGON WEIGHTS (GAUGE WEIGHT)

The Thiessen polygon map as shown in the Figure 5.3 was prepared using the tool "Thiessen polygon", available in ArcGIS software. The geographical coordinates of each rain gauge were supplied as input to the software. There are eleven rain-gauge stations. Out of eleven rain gauge stations, six stations have hourly rainfall values whereas others 5

stations have daily rainfall. The daily rainfall were converted to hourly rainfall. Thus the locations of those eleven rain gauge stations available of three storm events were considered for preparing this map. Table 5.1 provides gauge weights computed using the ArcGIS software. The computed Thiessen Gauge Weights of all the eleven rain gauge stations were considered as input to the HEC-HMS programme under its Meteorological Model to compute the average hourly rainfall over the basin for all three storm events.

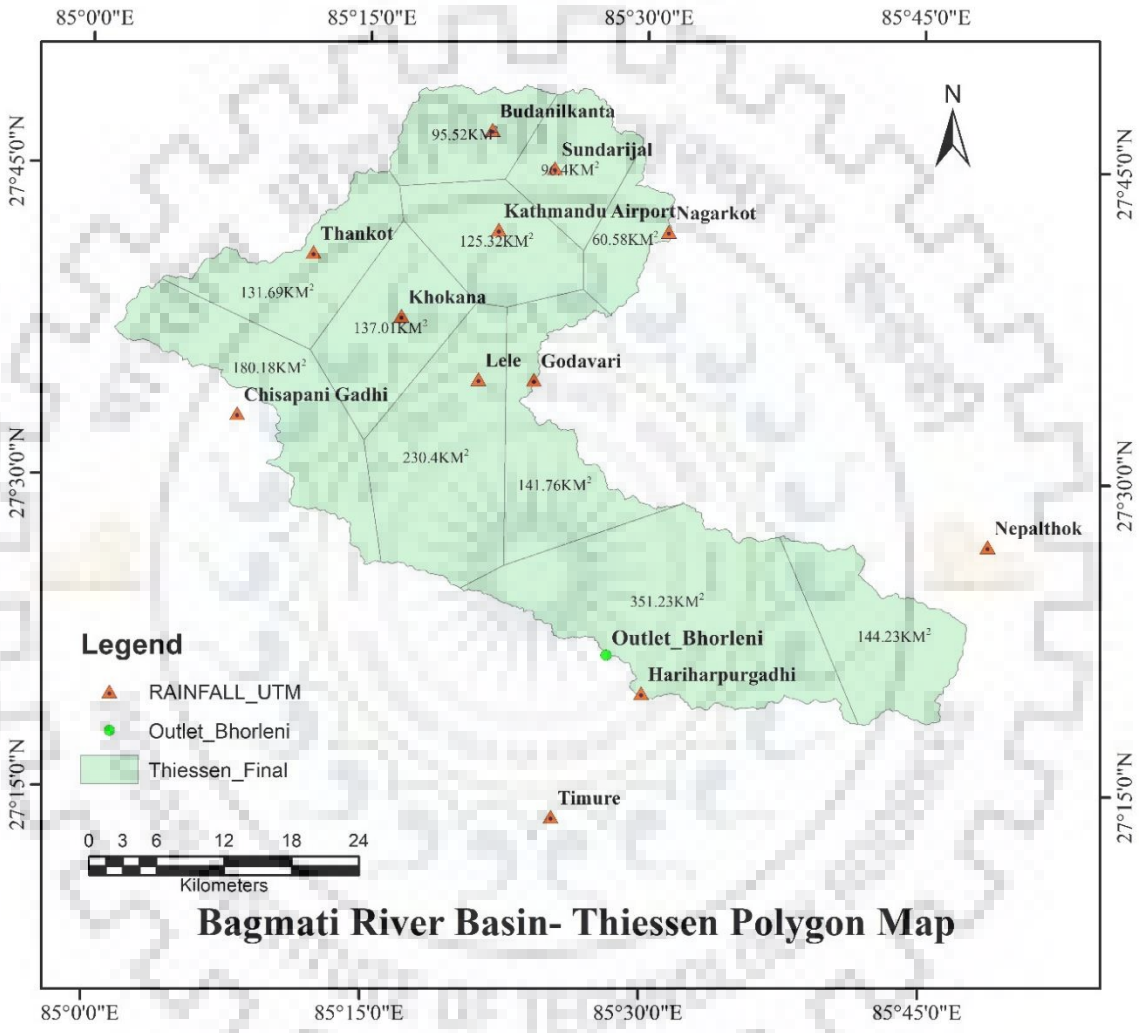

Figure 5.3 Thiessen Polygon Map of Bagmati River Basin up to Bhorleni Gauging Site

Table 5.1 Gauge Weights from Thiessen Polygon

Rainfall Station	Elevation	Coordinates		Thiessen Gauge Weight	
	RL	LAT	LONG	Area (sq.km)	Weightage factor
Budanilkanta	1350	27.78	85.36	95.52	0.06
Chisapani Gadhi	1706	27.55	85.13	180.18	0.11
Godavari	1400	27.58	85.40	141.76	0.08
Hariharpurgadhi	250	27.33	85.50	351.23	0.21
Kathmandu Airport	1337	27.7	85.37	125.32	0.07
Khokana	1212	27.63	85.28	137.01	0.08
Lele	1590	27.58	85.35	230.4	0.14
Nagarkot	2163	27.7	85.52	60.58	0.04
Nepalthok	1098	27.45	85.81	144.23	0.09
Sundarijal	1490	27.75	85.42	96.4	0.06
Thankot	1630	27.68	85.20	131.69	0.08
				1694.32	**1**

5.1.4 Preparation Of Land Use / Land Cover Map (LULC)

The LULC map was prepared using the "clip: tool of ARCGIS for extracting the LULC map for the basin from International Centre for Integrated Mountain Development (ICIMOD) (http://rds.icimod.org) where such maps are available in digital form. The map was taken of the year 2010 containing 7 different color band combinations. From the Figure 5.4, it is observed that the river basin is predominantly covered by the forest with 59.17 % of the basin area whereas the basin is covered with built up area and water body by 10.15% and 0.26% of the basin area respectively. The percentage areas covered by different land use land cover classes are given in Table 5.2. The percent area of the built up area (urban) represents the imperviousness in the basin. Accordingly, it was considered as one of the input for the loss model during HEC-HMS application.

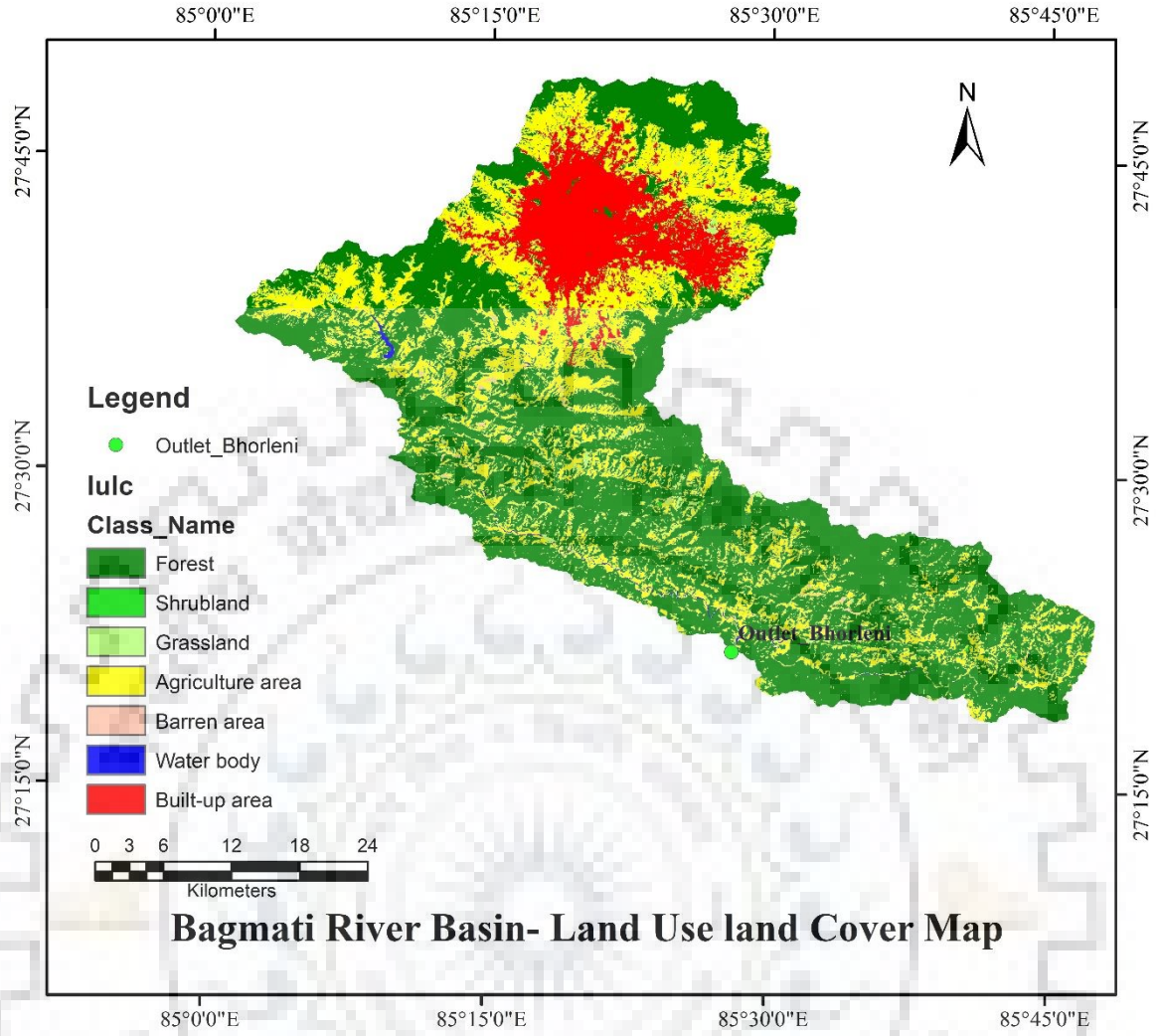

Figure 5.4 Land use land cover map of Bagmati River Basin upto Bhorleni Gauging Site

Table 5.2 Description of Land Use Land Cover

S.N	Class of Land use	Area in SQKM	Area in Percent
1	Forest	1002.41	59.17
2	Shrub land	1.64	0.10
3	Grassland	35.18	2.08
4	Agriculture area	473.49	27.95
5	Barren area	5	0.30
6	Water body	4.36	0.26
7	Built-up area	171.96	10.15
		1694.04	**100.00**

5.1.5 Preparation Of Isochrones Map And Development Of Time Area Relationship

The isochrones map was prepared using Inverse Distance Weighted (IDW) interpolation method. The longest flow path and river reaches were identified using HEC-GeoHMS software. Figure 5.5 shows the longest flow path and river reaches. The physical characteristics of the known river segments are given in the Table 5.3.

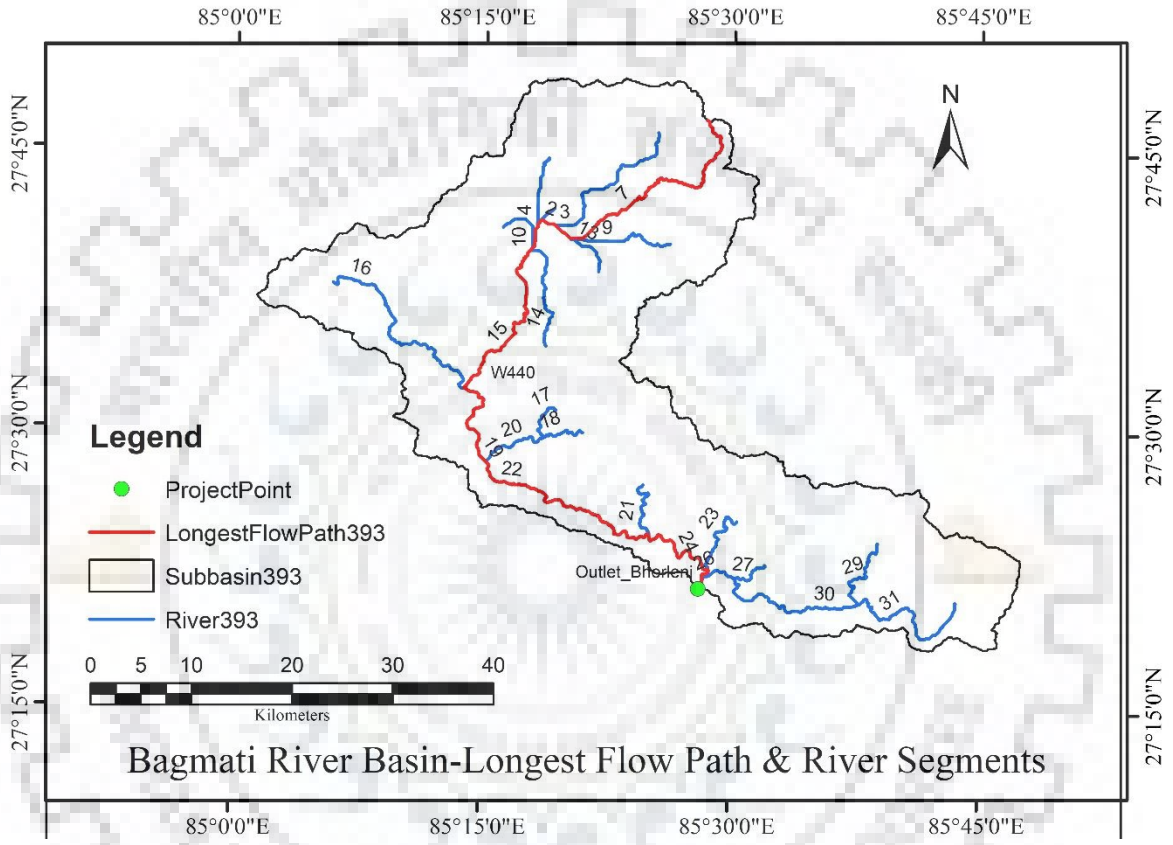

Figure 5.5 Figure: Longest Flow Path and River Reaches

Table 5.3 Physical Characteristics of River Reaches

River Reaches	Length of the River (L) in m	Slope (S)	L/√S
1	1819.61	0.001099	54888.33
2	1648.43	0.001213	47330.30
3	18053.93	0.015066	147086.51
4	7692.38	0.00143	203419.66
5	810.55	0.001234	23074.01
6	1965.21	0.00113	58461.35
7	15487.24	0.003228	272588.37
8	124.79	0.00213	2703.99
9	11507.74	0.002172	246922.12
10	5718.67	0.008394	62418.08
11	2266.13	0.005295	31142.35

12	332.79	0.048079	1517.70
13	5284.77	0.002649	102679.82
14	12637.16	0.013452	108957.21
15	20589.43	0.012336	185377.59
16	24962.18	0.028082	148959.60
17	4959.12	0.062108	19898.99
18	5634.79	0.051289	24880.85
19	11490.61	0.026804	70184.84
20	7963.49	0.037672	41029.29
21	8293.57	0.056188	34988.06
22	23645.57	0.013364	204541.53
23	9531.24	0.048682	43198.17
24	10638.46	0.010058	106077.43
25	1624.06	0.014778	13359.62
26	4163.28	0.008647	44771.60
27	4771.50	0.032904	26304.51
28	1062.66	0.011292	10000.24
29	10155.22	0.03545	53936.29
30	17541.45	0.00895	185418.91
31	17578.97	0.018147	130494.17

The maximum value of $\sum$ (L/√S) is found from the Table 5.4. Thus, the L/√S for the longest flow path from the catchment characteristics is estimated as 617653.18. Then value for constant C is determined from equation (4.3).

Table 5.4 Details of Points Located On the River and Its Tributaries and Time of Travels Up To the Gauging Site

Points	Summation of (L/√S) VALUE	Time of Travel to the Outlet t=C.∑(L/√S)	Longitude (East)	Latitude (North)
A	527804.7422	10.25	85.36	27.64
B	607426.1682	11.80	85.44	27.67
C	617653.1836	12.00	85.45	27.72
D	486230.8679	9.45	85.42	27.77
E	409200.0702	7.95	85.32	27.70
F	478464.4329	9.30	85.42	27.77
G	383426.9701	7.45	85.27	27.68
H	408280.939	7.93	85.31	27.58
I	328023.1225	6.37	85.10	27.63
J	218023.3919	4.24	85.32	27.52
K	220773.8534	4.29	85.35	27.50
L	90777.48297	1.76	85.41	27.45
M	36745.77833	0.71	85.51	27.42
N	204649.4946	3.98	85.73	27.35
O	132604.7301	2.58	85.65	27.40
P	44761.11803	0.87	85.53	27.38

Inverse Distance Weighted (IDW) Interpolation Method (Using ArcGIS): These isochrones were drawn using inverse distance weighted (IDW) interpolation technique of ArcGIS which helps to interpolate a raster surface from points with its known time of travel which is shown in Figure 5.6.

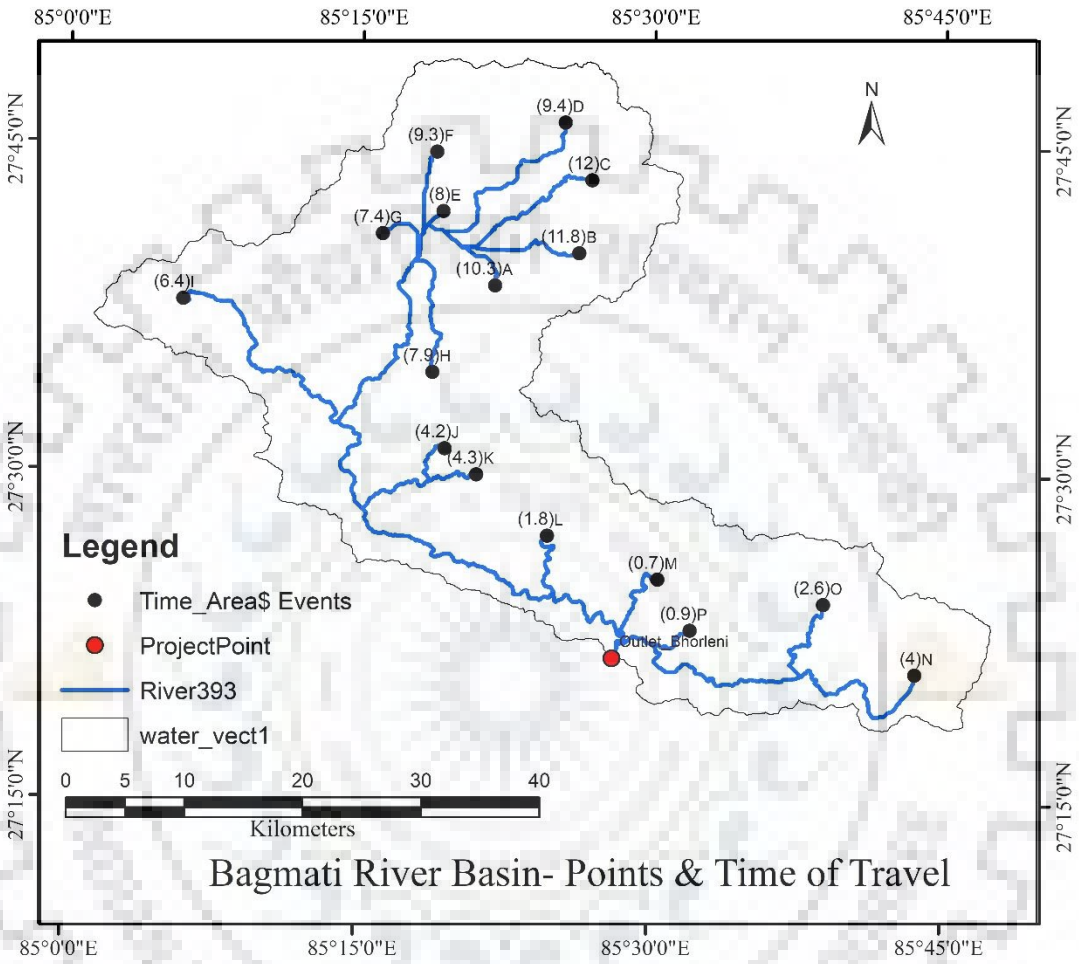

Figure 5.6 Points Located On the River and Its Tributaries and Its Time of Travel

The time of concentration (T_c) is considered as 12 hours during the computations. The Bagmati River Basin is divided into 12 different subareas enclosed between the two consecutive isochrones having time of one hour as shown in Figure 5.7. The time of travels associated with each isochrones and the area enclosed between the two consecutive isochrones were computed as given in Table 5.5. The cumulative area and time of travels are computed as given in Table. Subsequently, the value of t/Tc and At/A are computed. These values are also given in Table. The time area relationship obtained from this method was adopted in the Clark transform model of HEC-HMS.

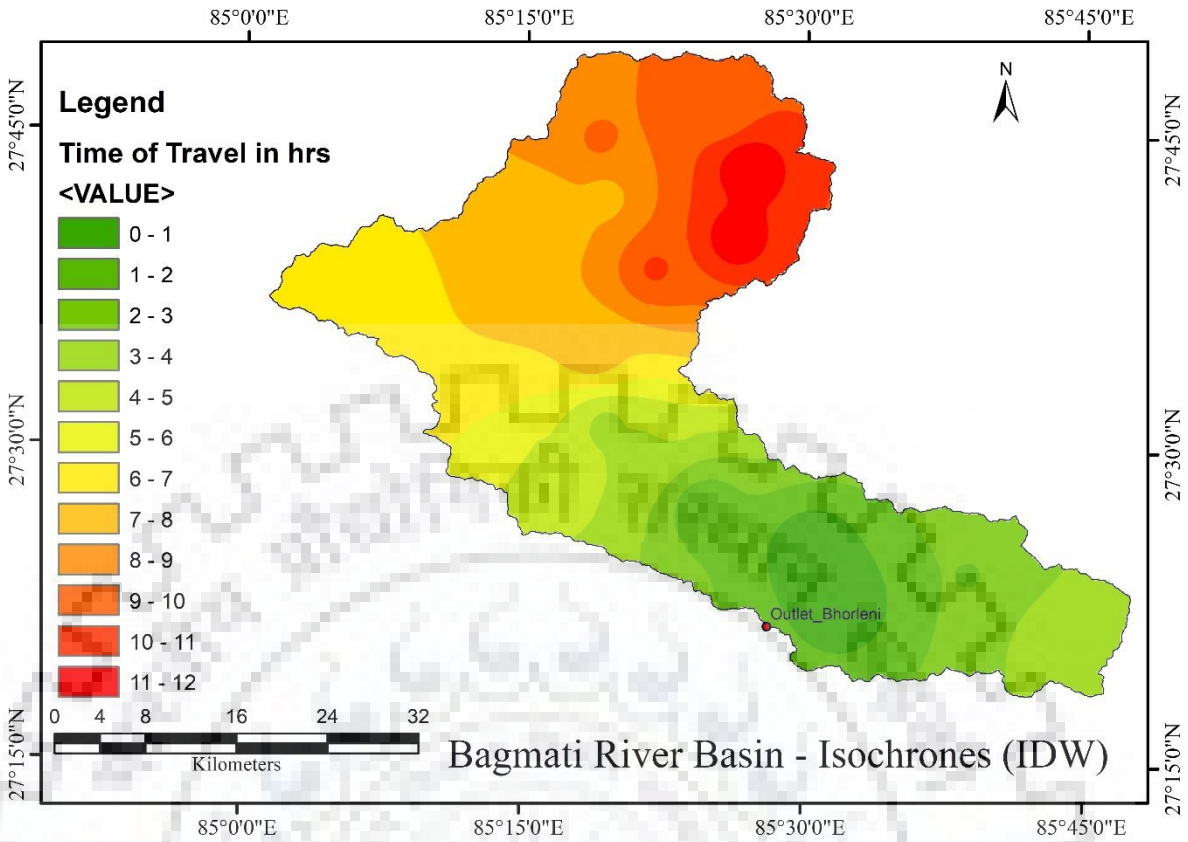

Figure 5.7 Isochrones of Bagmati River Basin (IDW)

Table 5. 5 Time Area Table of IDW Interpolation Method

Time of Travel between two consecutive isochrones	Area enclosed between two isochrones (SqKm)	Cumulative time of travel, Tc in Hr	Cumulative area, At in Sqkm	t/Tc	At/A
0-1	97.24	1	97.24	0.08	0.06
1-2	147.62	2	244.86	0.17	0.14
2-3	189.86	3	434.72	0.25	0.26
2-4	154.93	4	589.65	0.33	0.35
4-5	118.18	5	707.83	0.42	0.42
5-6	83.45	6	791.28	0.50	0.47
6-7	216.76	7	1,008.04	0.58	0.60
7-8	252.06	8	1,260.10	0.67	0.74
8-9	138.81	9	1,398.91	0.75	0.83
9-10	131.19	10	1,530.10	0.83	0.90
10-11	95.11	11	1,625.21	0.92	0.96
11-12	68.89	12	1,694.10	1.00	1.00

Table 5.5 was used to develop the time-area diagram and the time-area percent curve of the river basin as shown in Figure 5.8 & Figure 5.9. The time-area diagram or time-area percent curve represents the time of concentration that is consumed by the basin area up to the outlet of Bhorleni.

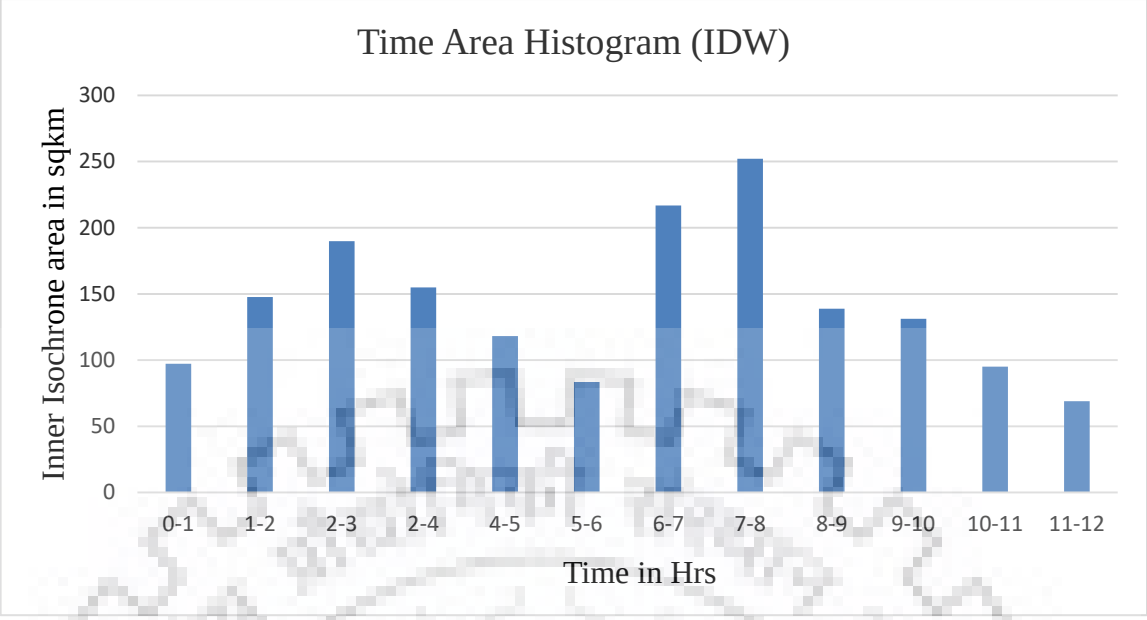

Figure 5.8 Time-Area Histogram - IDW

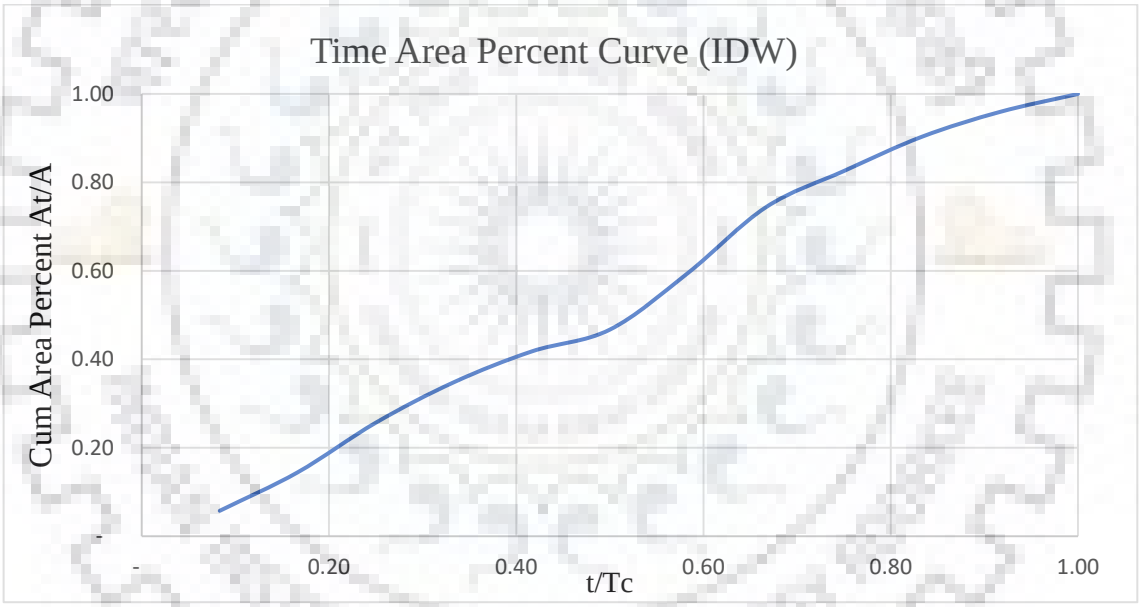

Figure 5.9 Cumulative Time-Area Percent Curves- IDW

5.2 TEMPORAL DATA PROCESSING

5.2.1 RAINFALL DATA PROCESSING

The storm events in Table 5.6 were considered for rainfall runoff modelling using HEC-HMS. The hourly rainfall values were recorded at eleven rain gauge stations for all the storm events of the Bagmati River basin. To compute the average hourly rainfall for each event, Thiessen polygon weight factors of those eleven rain gauge stations were used in HEC-HMS programme. The computations of those gauge weights were already discussed in section 5.1.3.

Table 5.6 Storm Events Considered For HEC-HMS Modeling

Storm Events	Duration in Hours
2 July 2018 - 4 July 2018	48
12Aug 2018 - 14 Aug 2018	50
11 July 2018 - 14 July 2018	54

5.2.2 STREAM FLOW DATA PROCESSING

The stream flow data i.e. measured discharge is key for adjustment and approval of the formulated model in HEC-HMS for calibration and validation purposes. The hourly stream flow data at Bhorleni gauge station is collected from Hydrology section of the Department of Hydrology and Meteorology (DHM), Nepal.

5.3 APPLICATION OF HEC-GEO-HMS AND HEC-HMS

The basin model of the Bagmati River Basin including required physical characteristics of the basin was processed using the software HEC-GeoHMS as shown in Figure 5.10. Further, the element networks of the basin to be represented in the HEC-HMS desktop also was developed using the software HEC-GeoHMS as shown in the Figure 5.10. For this processing, DEM of the study area was used as raw data in the software HEC-GeoHMS. Then, the processed Bagmati River Basin Model with element networks was imported to the HEC-HMS desktop as shown in the Figure 5.11. Further, the components of HEC-HMS and the description of the project used in HEC-HMS programme are also displayed in watershed explorer and component editor respectively as shown in the Figure 5.11.

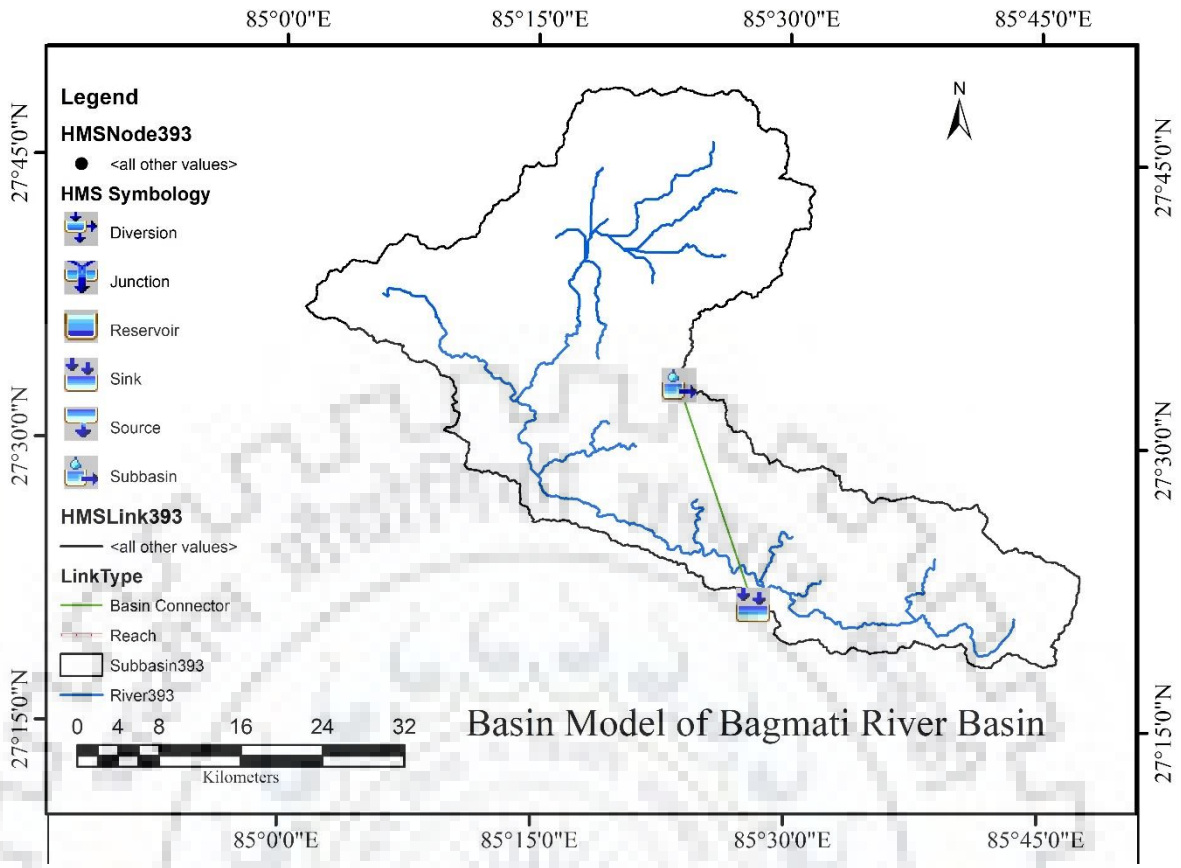

Figure 5.10 Basin Model processed in HEC-GeoHMS

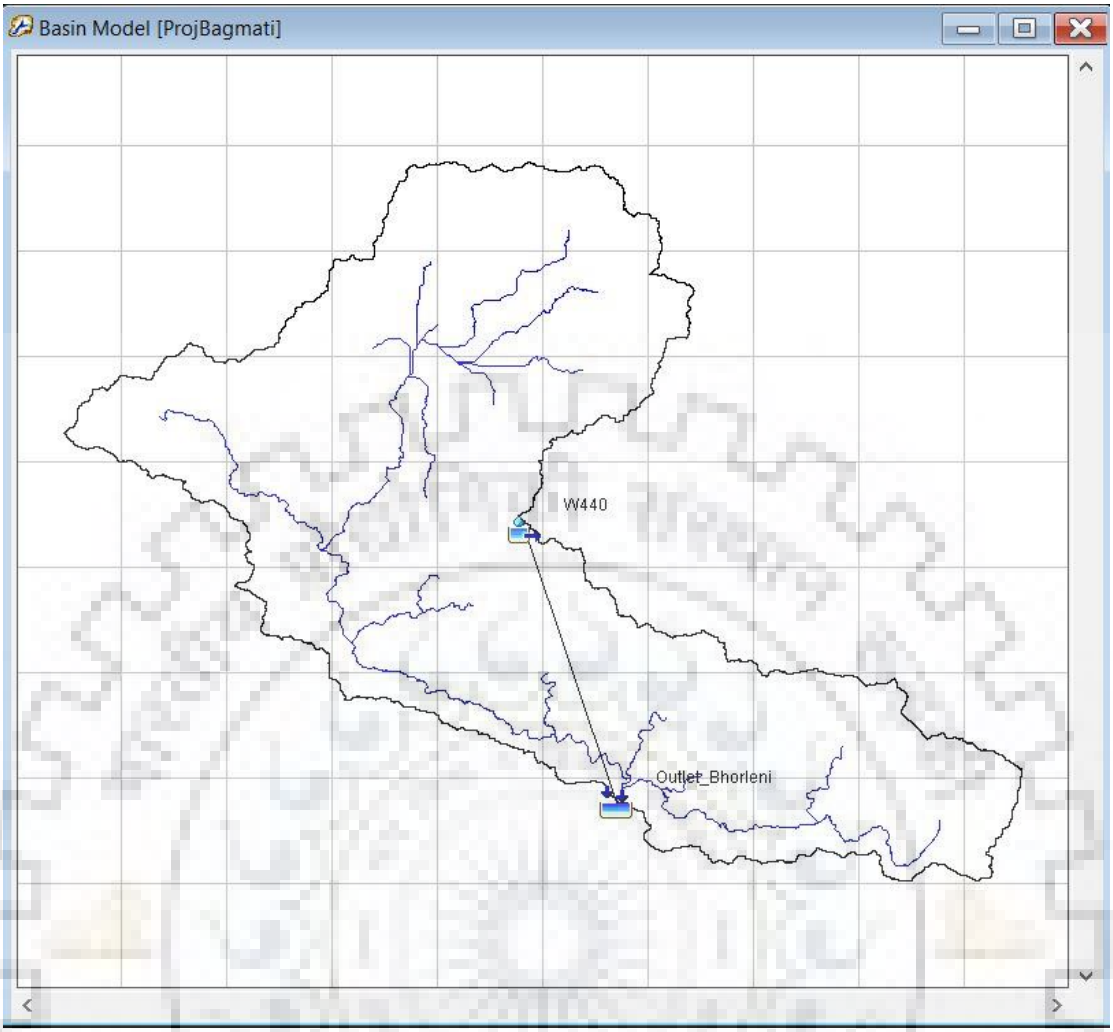

Figure 5.11 Model used in HEC-HMS for Event 2 July 2018- 4 July 2018

5.3.1 METEOROLOGICAL MODEL

The Thiessen polygon weights already computed were used under the meteorological model of HEC-HMS programme. The component editor displays the table containing those Thiessen polygon weights as shown in Table 5.7. Thus, the average hourly rainfall computed for the event 2 July 2018- 4 July 2018 is displayed in the results preview as shown in Figure 5.12.

Table 5.7 Thiessen Polygon Weights For HEC-HMS Modeling

S.N	Name of Gage Stations	Depth Weight	Time Weight
1	Budanilkanta	0.06	1
2	Chisapani Gadhi	0.11	1
3	Godavari	0.08	1
4	Hariharpurgadhi	0.21	1

5	Kathmandu Airport	0.07	1
6	Khokana	0.08	1
7	Lele	0.14	1
8	Nagarkot	0.04	1
9	Nepalthok	0.09	1
10	Sundarijal	0.06	1
11	Thankot	0.08	1

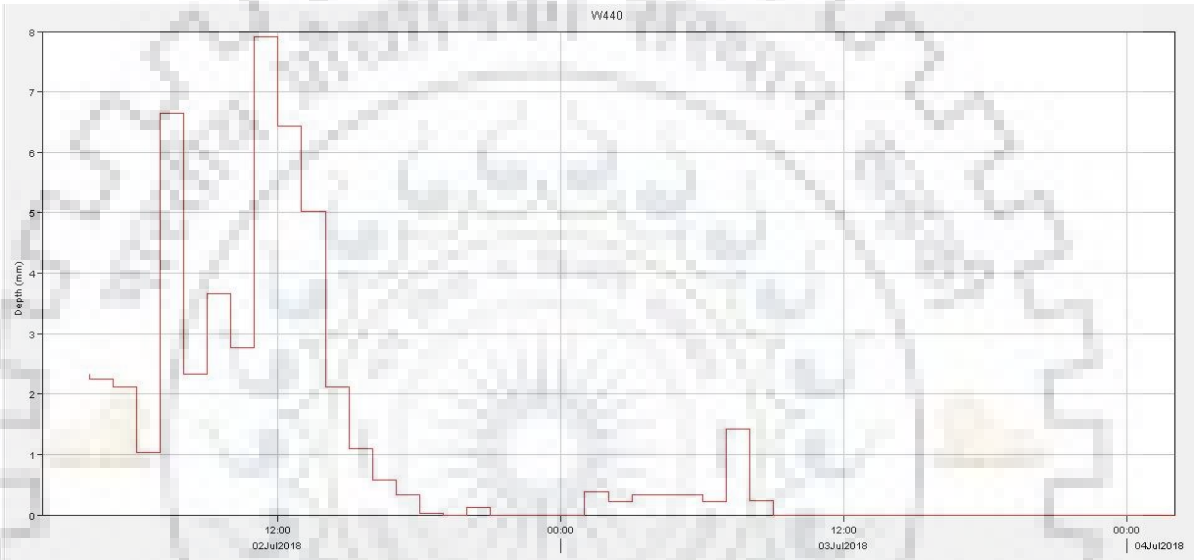

Figure 5.12 Output of Rainfall in HEC-HMS for Event 2 July 2018- 4 July 2018

5.3.2 BASE FLOW MODEL

The direct surface runoff hydrographs are computed separating the base flow from the observed flood hydrograph for each flood events using recession method. For this method of base flow separation, the initial value of the recession constant was derived as 0.1 whereas the initial discharge and threshold type (Ratio to Peak) are obtained as 100 m^3/s and 0.1 respectively from the observed flood hydrograph as base flow model initial parameters during the optimization in HEC-HMS programme. The variation in base flow with the time is shown in the results preview in Figure 5.13.

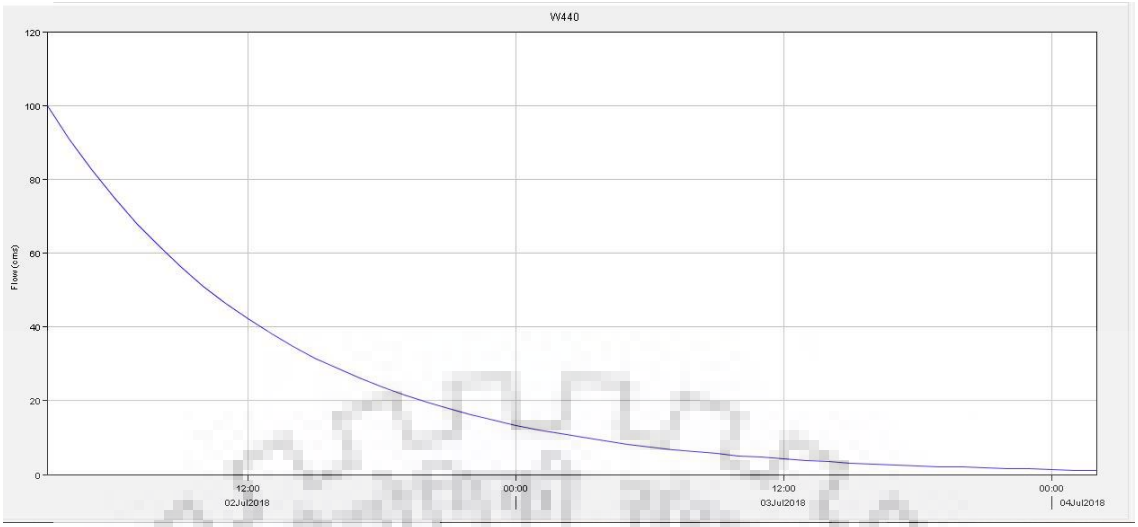

Figure 5.13 Output as Base Flow in HEC-HMS for the Event 2 July 2018- 4 July 2018

5.3.3 LOSS MODEL

Initial loss and constant rate method were chosen as loss model and the corresponding values of that loss parameter are 0.3 mm and 0.9 mm/hr. used in the HEC-HMS. From these parameter values, the variation of soil infiltration with time was simulated in the HEC-HMS programme as shown in Figure 5.14. These soil infiltration values were subtracted from the average rainfall to compute the excess rainfall. The excess rainfall computed within the HEC-HMS programme is shown in Figure 5.15.

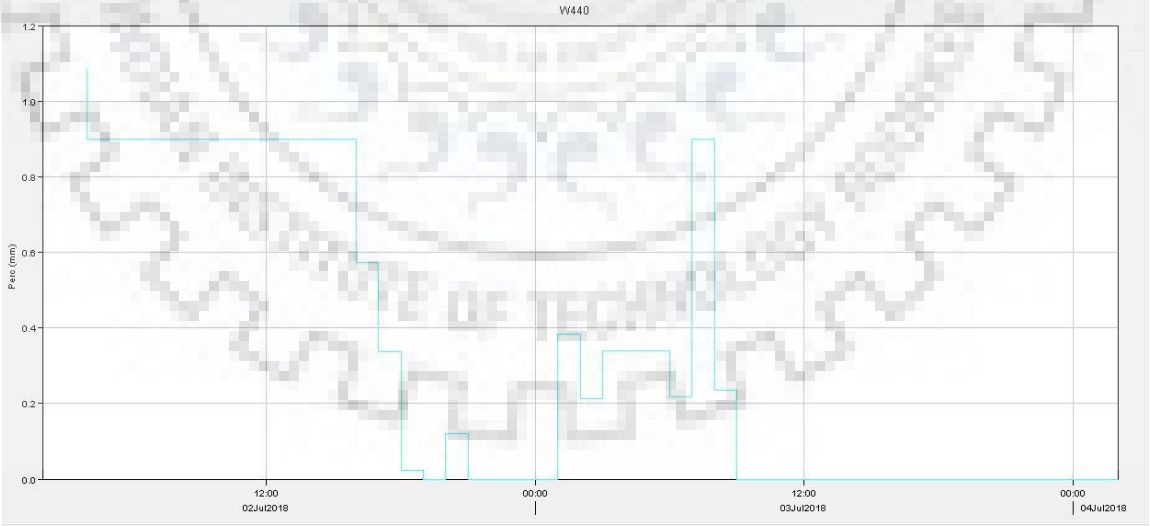

Figure 5.14 Output as Soil Infiltration in HEC-HMS for the Event 2 July 2018- 4 July 2018

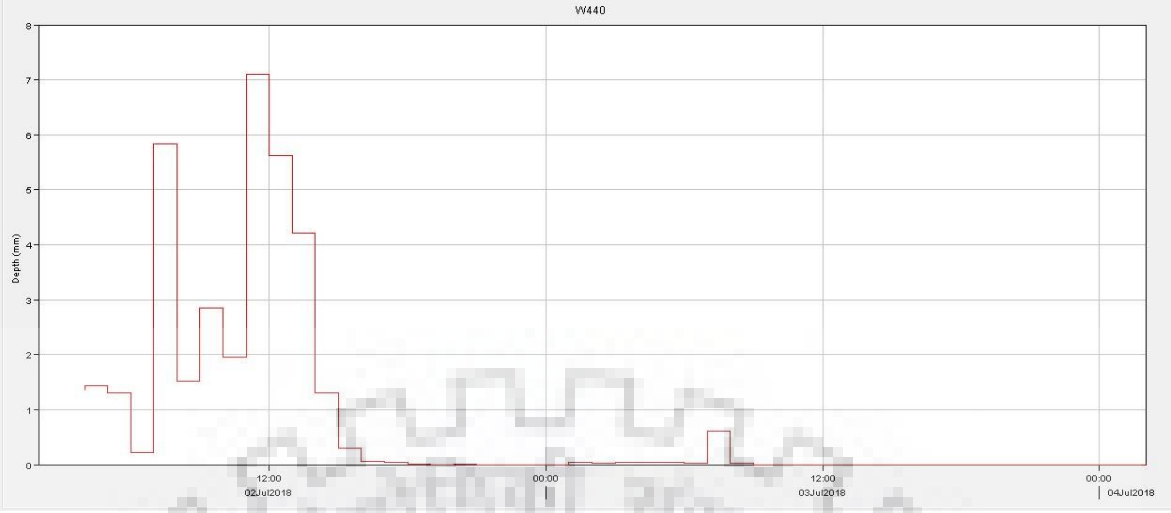

Figure 5.15 Output of Excess Rainfall in HEC-HMS for Event 2 July 2018- 4 July 2018Transform Model

5.3.4 TRANSFORM MODEL

5.3.4.1 CLARK UH MODEL

The initial values of the parameters Time of Concentration, Tc and Storage of Coefficient, R for Clark model were taken as 4 hrs and 29 hrs respectively during optimization of the event 2 July 2018- 4 July 2018. The time area percent curve, considered as the input for Clark model was used in the HEC-HMS programme as shown in the Figure 5.16. Finally, the direct runoff hydrograph for the event 2 July 2018- 4 July 2018, was computed under Clark model by running the HEC-HMS programme as shown in Figure 5.17.

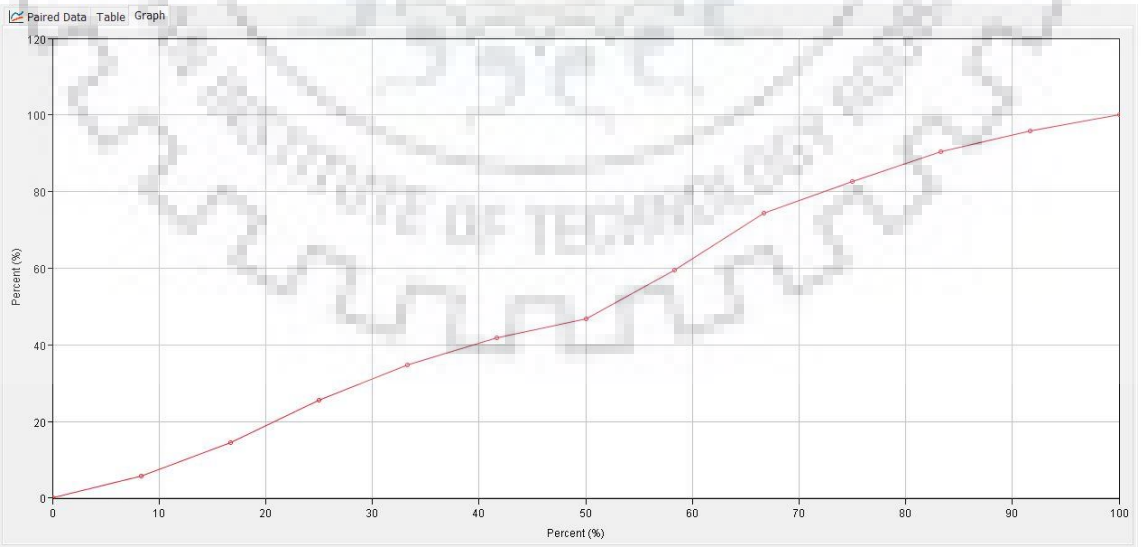

Figure 5.16 Time Area Percent Curve used in Clark UH Model of HEC-HMS

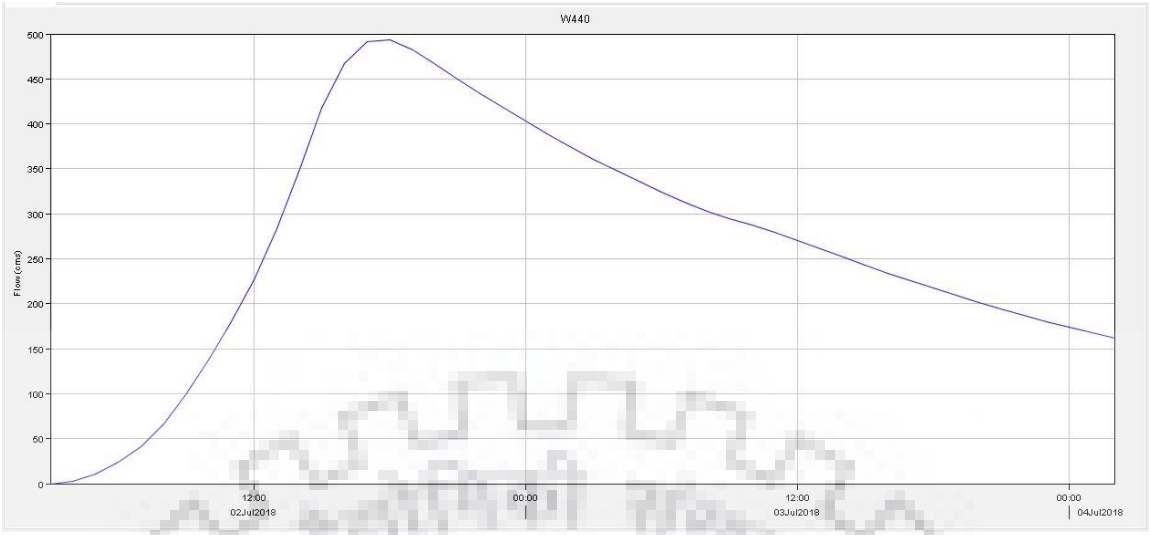

Figure 5.17 Output of Direct Runoff (Clark UH) in HEC-HMS for Event 2 July 2018- 4 July 2018

5.3.4.2 SNYDER UH MODEL

The initial values of the parameters Peaking coefficient, C_p as 0.11 and Standard lag, t_p as 4 hrs were taken during the optimization for the event 2 July 2018- 4 July 2018 under Snyder model. Finally, the direct runoff hydrograph for the event 2 July 2018- 4 July 2018 was computed for Snyder model by running the HEC-HMS programme for optimization option as shown in the Figure 5.18.

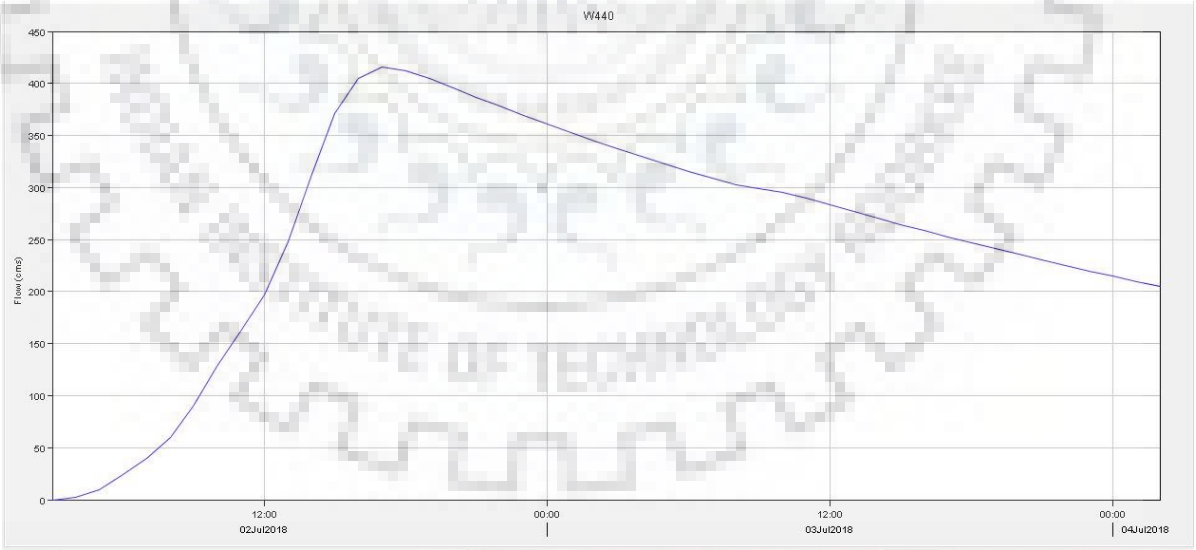

Figure 5.18 Output of Direct Runoff (Snyder UH) in HEC-HMS for Event 2 July 2018- 4 July 2018

5.4 SENSITIVITY ANALYSIS

The sensitivity analysis of transform model: Clark and Snyder models was carried out. The NSE values for the various sets of Tc and R parameters were determined during simulation of the storm event 2 July 2018- 4 July 2018 and those NSE values are given in Table 5.8. The computed NSE values, corresponding to a set of Tc and R values were plotted and contours for NSE values were drawn. The NSE contours drawn are shown in Figure 5.19. The initial values of parameters Tc and R were identified from highest range of NSE contour. The initial values of parameters Tc and R were values, obtained from sensitivity analysis, were considered as 4 hrs and 29 hrs respectively for computing the optimum values of Tc and R using HEC-HMS.

Table 5.8 Parameters Tc and R on Sensitivity Analysis

Storage Coefficient, R (Hrs.)	8	16	24	32	40	48
Time of Concentration Tc (Hrs.)	Nash-Sutcliffe Model Efficiency Coefficient					
2	-6.793	-0.817	0.577	0.882	0.832	0.65
4	-5.839	-0.544	0.662	0.895	0.881	0.611
6	-5.042	-0.391	0.653	0.833	0.729	0.52
8	-4.366	-0.344	0.563	0.704	0.589	0.38
10	-3.865	-0.39	0.41	0.528	0.413	0.208
12	-3.5	-0.5	0.218	0.325	0.215	0.02

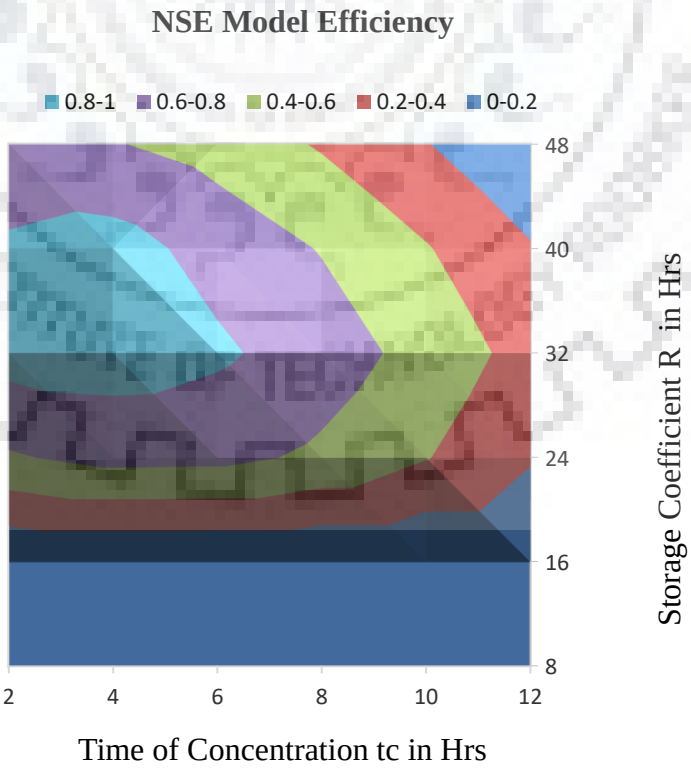

Figure 5.19 Contour of NSE model efficiency with Sensitive Parameters Tc & R

The NSE values, corresponding to the various sets of peaking coefficients, C_p and standard lag, t_p parameters were estimated during simulation of the storm event 2 July 2018- 4 July 2018 as given in the Table 5.9. NSE values are plotted corresponding to the peaking coefficient, C_p and standard lag, t_p and contours of NSE values were drawn as shown in Figure 5.20. The initial values of peaking coefficients, C_p and standard lag, t_p were identified from highest range of NSE contour. Thus the initial values of peaking coefficients, C_p and standard lag, t_p were considered as 0.11 and 4 hrs respectively for optimizing these parameters using HEC-HMS.

Table 5.9 Parameters Standard Lag And Cp on Sensitivity Analysis

Standard Lag tp (hrs)	2	4	6	8	10
Peaking Coefficient Cp	Nash-Sutcliffe Model Efficiency Coefficient				
0.1	-0.68	0.748	0.32	-0.334	-0.934
0.2	-5.885	-0.27	0.717	0.671	0.326
0.3	-12.52	-2.975	-0.33	0.404	0.47
0.4	-18.39	-6.535	-2.264	-0.598	-0.034
0.5	-23.079	-10.609	-4.84	-2.159	-1.028

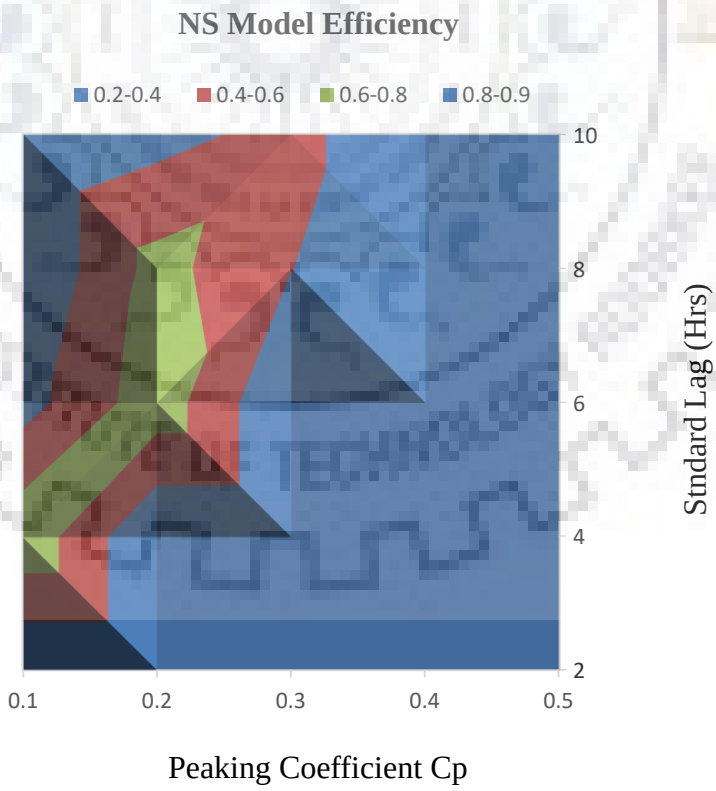

Figure 5.20 Variation of NSE with Sensitive Parameters C_p & Standard Lag (t_p)

5.5 ERROR CRITERIA FOR COMPARING THE PERFORMANCE OF MODEL

The error criteria for the performance of the transform models were considered as described under section 4.5. Out of those four criteria, *NSE* value was considered for evaluating the overall performance of the transform model during calibration and validation.

5.6 CALIBRATION AND VALIDATION

For the calibration of the transform models, two storm events data were considered whereas one storm event data was used for the validation for Bagmati River Basin up to Bhorleni gauging site. The details about these three storm events were given in Table 3.1. The initial values of hydrological parameters were obtained from the sensitivity analysis of the corresponding transform model whereas initial values of the other measured parameters were derived from the spatial data processing.

5.6.1 CALIBRATION OF CLARK UH MODEL

The Clark UH transform model was calibrated from two events. During the calibration of the Clark Model Parameters, the optimization option available in the simulation manager of HEC-HMS was used for the individual events to optimize the Clark UH model parameter such as Tc and R. The initial values of Tc and R, which were obtained from the sensitivity analysis, were used as 4 hr and 29 hr respectively. The optimized values of those parameters of the individual events including average values of those parameters are given in the Table 5.10 and the representative parameters of Clark model for the basin were computed taking the average of the optimized parameters obtained from analyzing the data of two storm events using HEC-HMS programme.

Table 5.10 Average Optimized Parameters – Clark UH Transform Model

Model	**Parameters**	**Events Considered for Calibration**		**Representative Parameters (Average Parameters)**
		2 July 2018 - 4 July 2018	**12Aug 2018 - 14 Aug 2018**	
Transform	Clark Unit Hydrograph - Time of Concentration in hrs	4	5	5
	Clark Unit Hydrograph - Storage Coefficient R in hrs	29	25	27

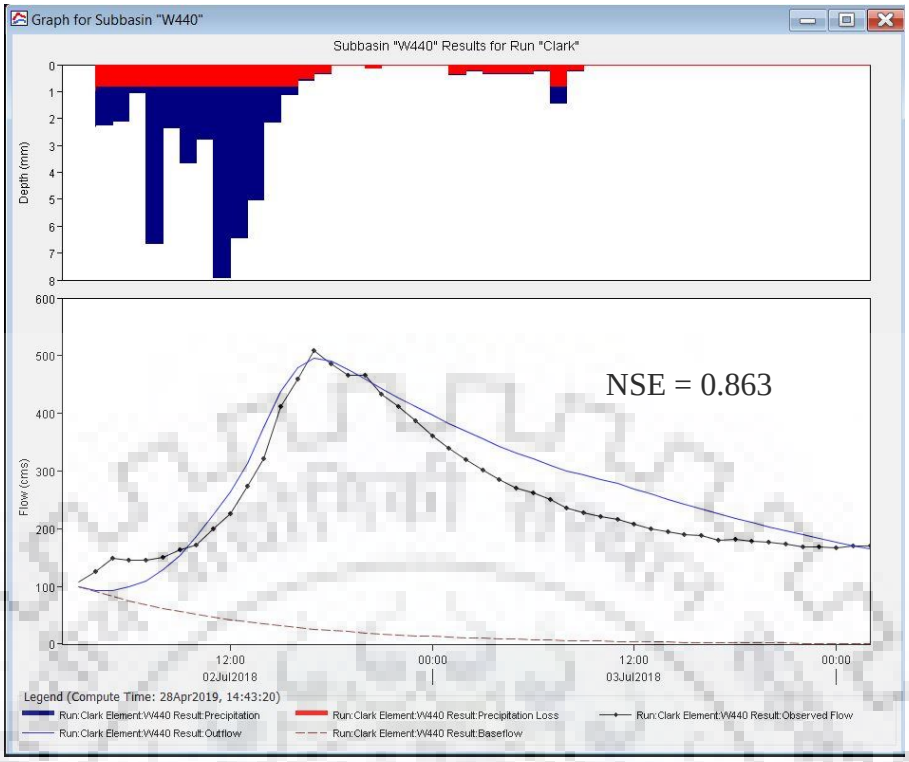

a) Event of 2 July 2018- 4 July 2018

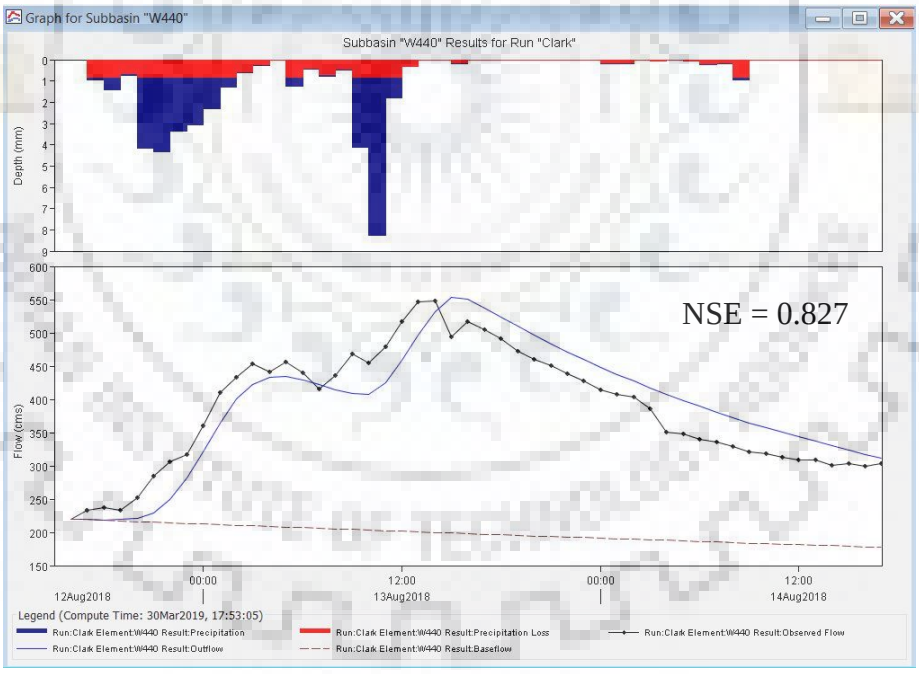

b) Event of 12 August 2018- 14 August 2018

Figure 5.21 Comparison of Observed and Simulated Flood Hydrograph using optimized parameters of Clark Model for all the two events considered for Calibration

The simulated flood hydrographs using the optimized parameters of Clark model are shown in the Figures 5.21 (a) and 5.21 (b) for two storm events. These Figures illustrate the comparison of observed flood hydrographs with the simulated flood hydrographs for

the two storm events. During calibration of these two events, the optimization option available in the simulation manager of HEC-HMS was individually used for the events to optimize the Clark UH model parameters such as Tc and R. The initial values of Tc and R, which were obtained from the sensitivity analysis, were used as 4hr and 29hr respectively. The optimized values of those parameters of the individual events including average values of those parameters are given in Table 5.10. From the Table, it is observed that the average value of optimized Tc (=5hrs) differs from its optimized value obtained from the two events whereas the average value of optimized R (=27hrs) is also slightly differ for the events.

Figure 5.22 shows the comparison of observed flood hydrograph with simulated flood hydrographs using optimized parameters and representative parameters (averaged parameters) of the Clark UH model for the event 2 July 2018 – 4 July 2018. From this figure, it is observed that NSE value (NSE=0.809) obtained from the representative parameters of the Clark model is lower than the NSE value (NSE=0.863) obtained from the optimized parameters of the Clark model.

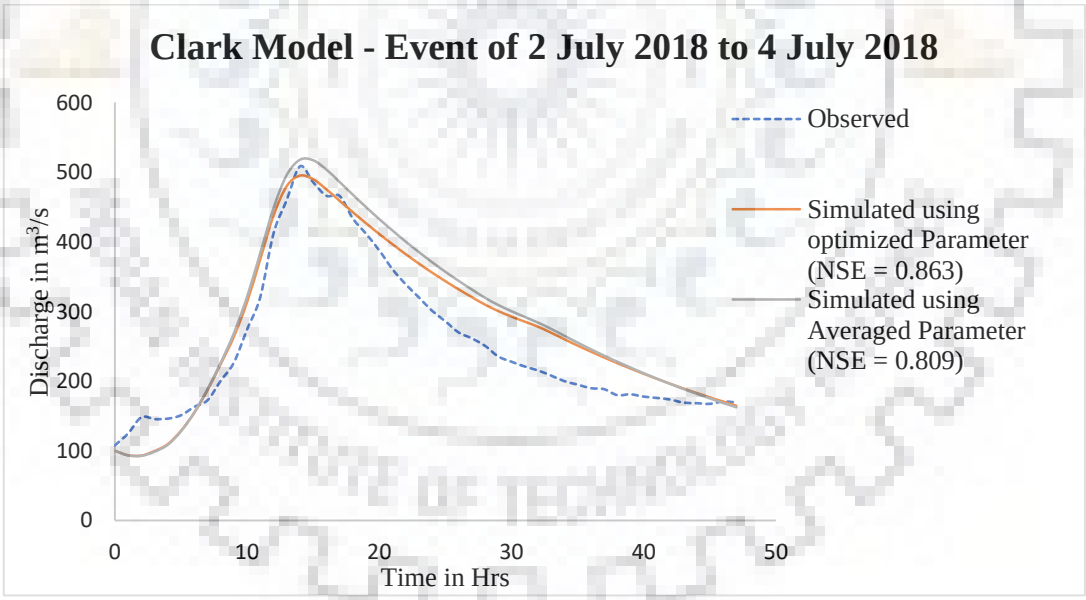

Figure 5.22 Comparison of Observed and Simulated Flood Hydrograph using optimized as well as representative parameters of Clark Model for event 2 July 2018 – 4 July 2018

Figure 5.23 shows the comparison of observed flood hydrograph with simulated flood hydrographs using optimized parameters and representative parameters (averaged parameters) of the Clark UH model for the event 12 August 2018 – 14 August 2018. From this figure, it is observed that NSE value (NSE=0.838) obtained from the representative

parameters of the Clark model is slightly equal to the NSE value (NSE=0.827) obtained from the optimized parameters of the Clark model.

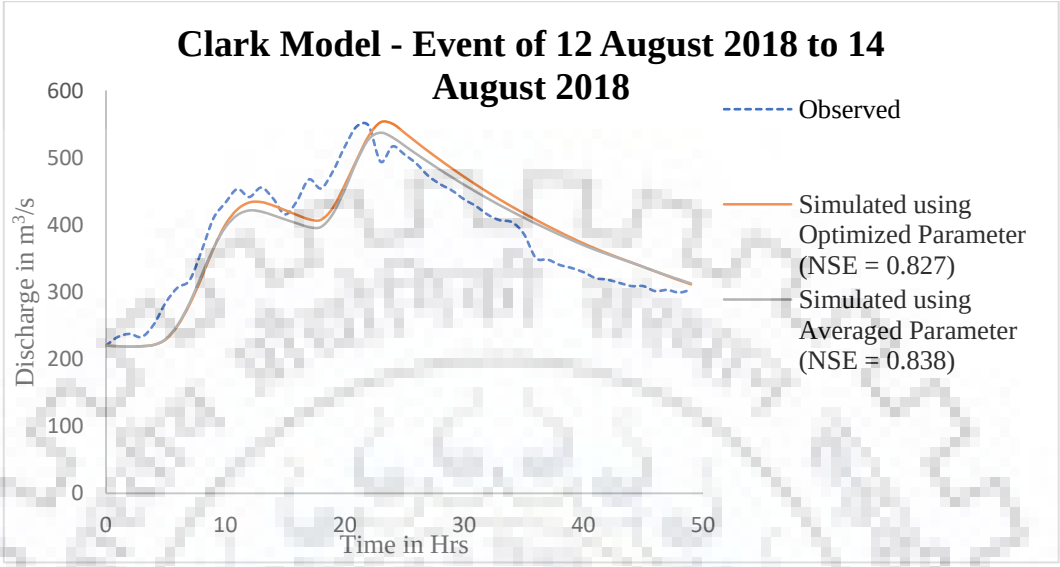

Figure 5.23 Comparison of Observed and Simulated Flood Hydrograph using optimized as well as representative parameters of Clark Model for event 12 August 2018 – 14 August 2018

5.6.2 CALIBRATION OF SNYDER UH MODEL

The Snyder UH transform model was calibrated from the two events. During the calibration of the Snyder Model Parameters, the optimization option available in the simulation manager of HEC-HMS was used for the individual events to optimize the Snyder UH model parameters such as C_p and T_p. The initial values of C_p and T_p, which were obtained from the sensitivity analysis were used as 0.11 and 4hrs respectively. The optimized values of those parameters of the individual events including average values of those parameters are given in Table 5.11. and the representative parameters of Snyder model for the basin were computed taking the average of the optimized parameters obtained from analyzing the data of two events using HEC-HMS programme.

Table 5.11 Average Optimized Parameters – Snyder UH Transform Model

Model	Parameters	Events Considered for Calibration		Representative Parameters (Average Parameters)
		2 July 2018 - 4 July 2018	12Aug 2018 - 14 Aug 2018	
Transform	Snyder Unit Hydrograph - Peaking Coefficient	0.11	0.18	0.15
	Snyder Unit Hydrograph - Standard Lag in hrs	4	5	4.5

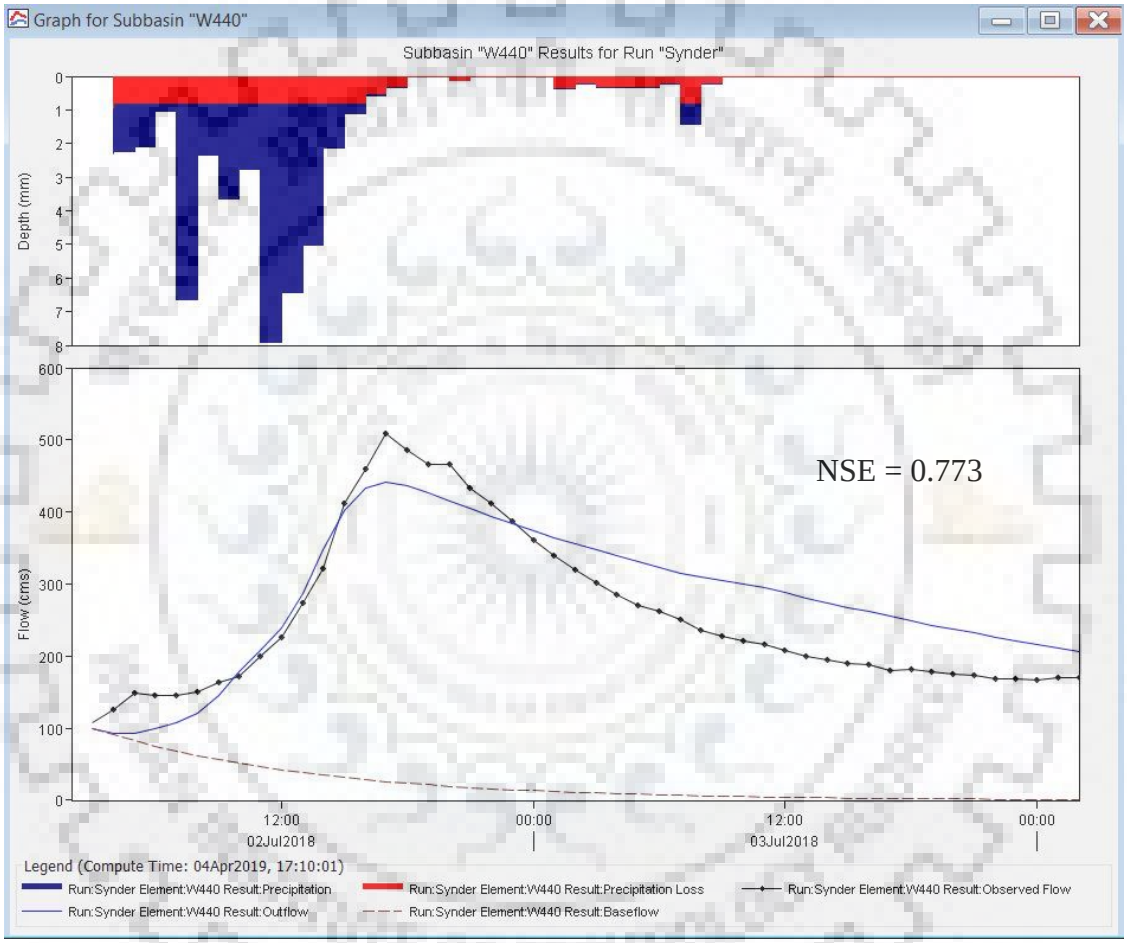

a) Event of 2 July 2018- 4 July 2018

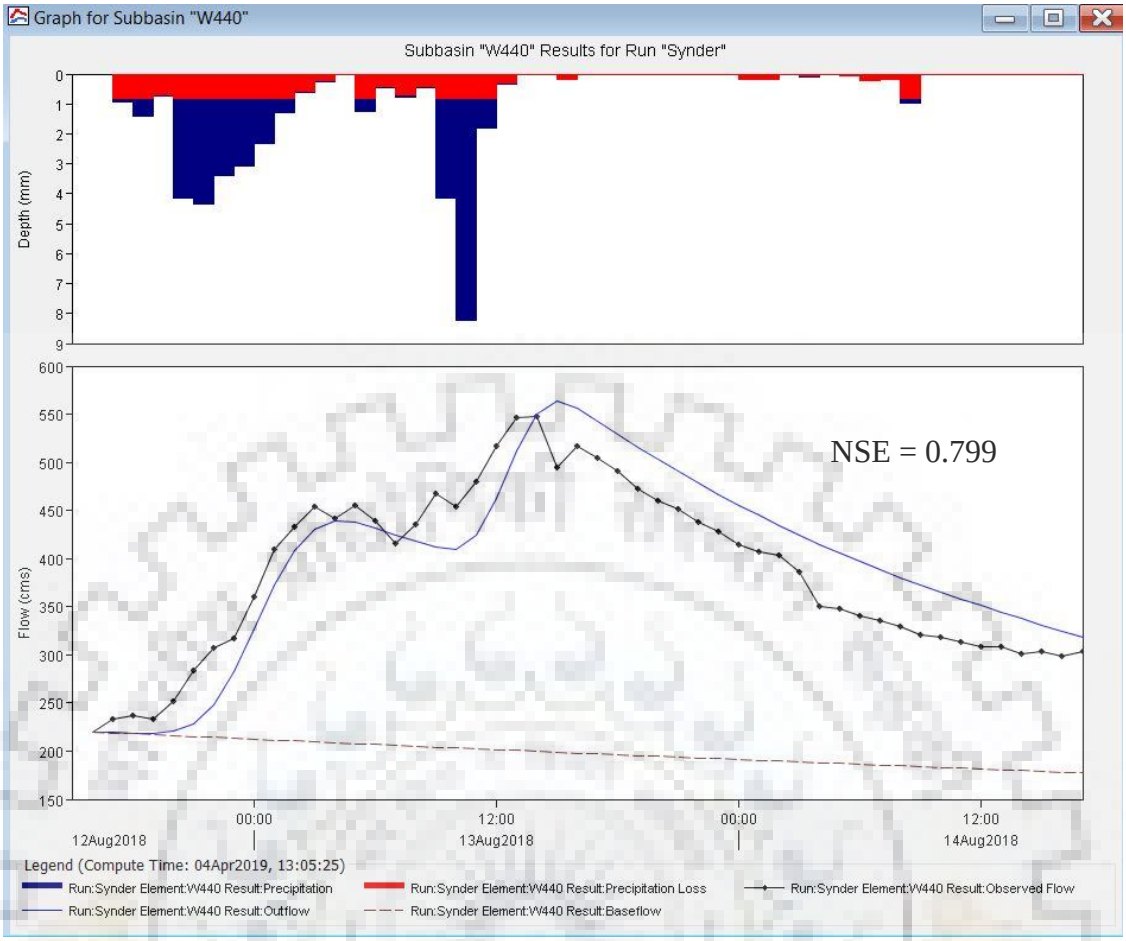

b) Event of 12 August 2018- 14 August 2018

Figure 5.24 Comparison of Observed and Simulated Flood Hydrograph using optimized parameters of Snyder Model for all the two events considered for Calibration

The simulated flood hydrographs using the optimized parameters of Snyder model are shown in the Figures 5.24 (a) and 5.24 (b) for two storm events. These Figures illustrate the comparison of observed flood hydrograph with the simulated flood hydrographs for the two storm events. During calibration of these two events, the optimization option available in the simulation manager of HEC-HMS was individually used for the events to optimize the Snyder UH model parameters such as C_p and t_p. The initial values of C_p and t_p, which were obtained from the sensitivity analysis, were used as 0.11 and 4hr respectively. The optimized values of those parameters of the individual events including average values of those parameters are given in Table 5.10. From the Table, it is observed that the average value of optimized C_p (=0.15) differs from its optimized value obtained from the two events whereas the average value of optimized t_p (=4.5hrs) is also slightly differ for the events.

Figure 5.25 shows the comparison of observed flood hydrograph with simulated flood hydrographs using optimized parameters and representative parameters (averaged parameters) of the Snyder UH model for the event 2 July 2018 – 4 July 2018. From this figure, it is observed that NSE value (NSE=0.736) obtained from the representative parameters of the Snyder model is lower than the NSE value (NSE=0.773) obtained from the optimized parameters of the Snyder model.

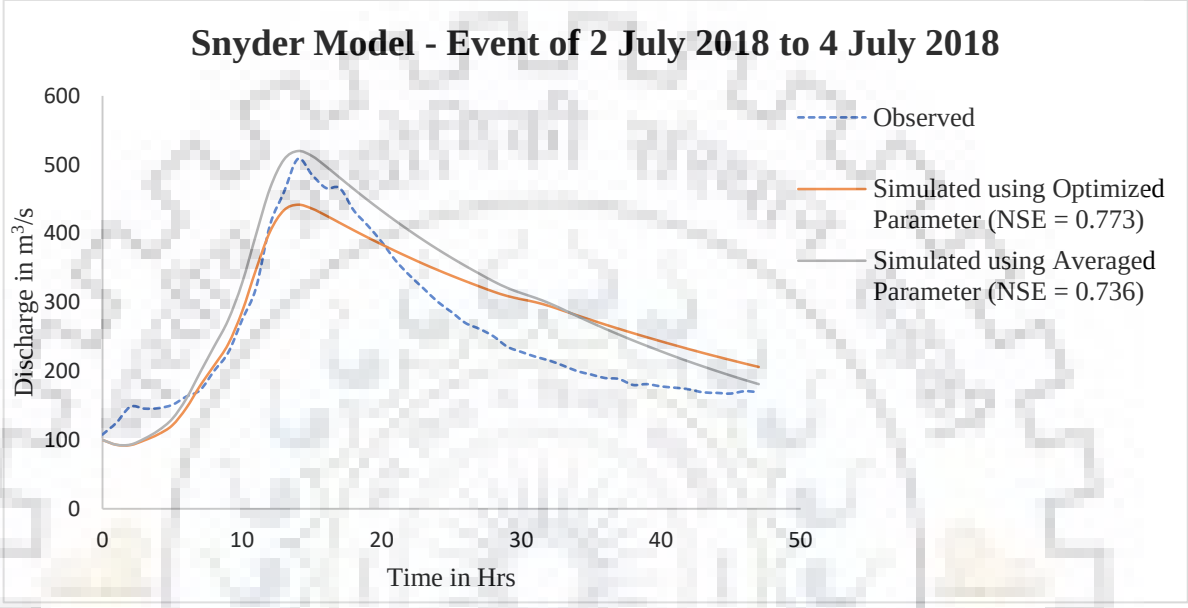

Figure 5. 25 Comparison of Observed and Simulated Flood Hydrograph using optimized as well as Averaged parameters of Snyder Model for event 2 July 2018 – 4 July 2018

Figure 5.26 below shows the comparison of observed flood hydrograph with simulated flood hydrographs using optimized parameters and representative parameters (averaged parameters) of the Snyder UH model for the event 12 August 2018 – 14 August 2018. From this figure, it is observed that NSE value (NSE=0.810) obtained from the representative parameters of the Snyder model is slightly equal to the NSE value (NSE=0.799) obtained from the optimized parameters of the Snyder model.

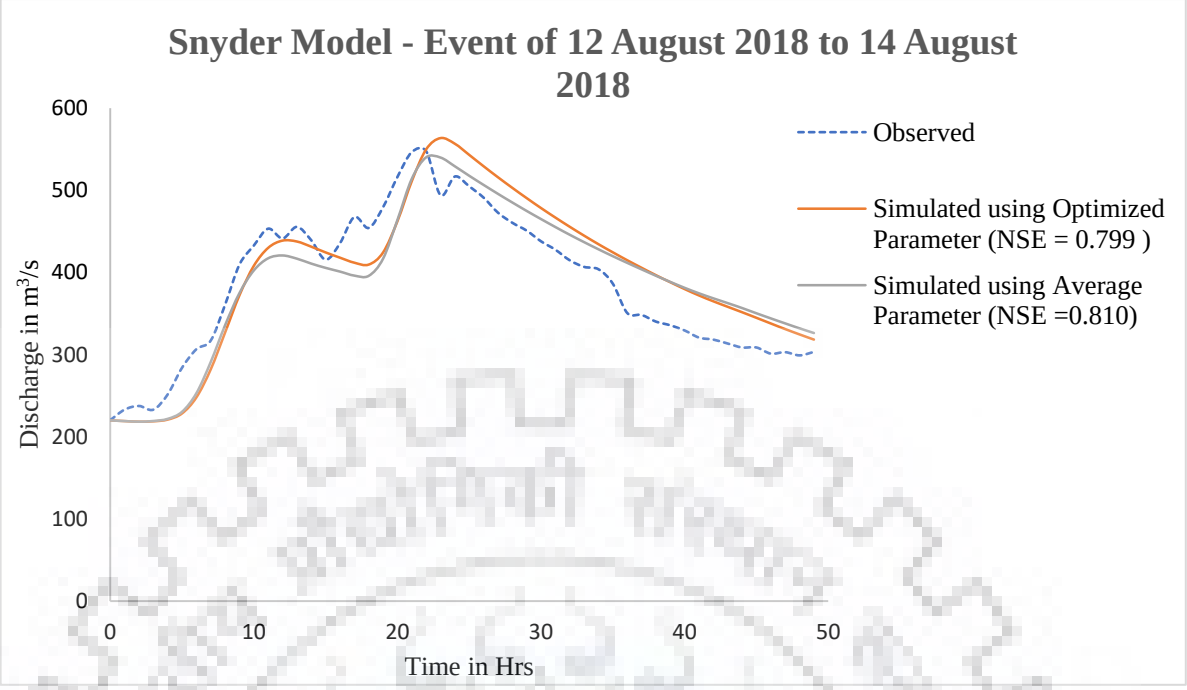

Figure 5.26 Comparison of Observed and Simulated Flood Hydrograph using optimized as well as Averaged parameters of Snyder Model for event 12 August 2018 – 14 August 2018

5.6.3 Comparison Of Two Transform Models During Calibration

Figure 5.27 shows the comparison of simulated flood hydrographs using representative parameters (averaged parameters) of the two transform model with the observed flood hydrograph for the event 2 July 2018 – 4 July 2018. From the figure, it is observed that the Clark UH transform model gave best performance with the NSE of 0.809 whereas the Snyder UH transform model have the performance with the NSE of 0.736.

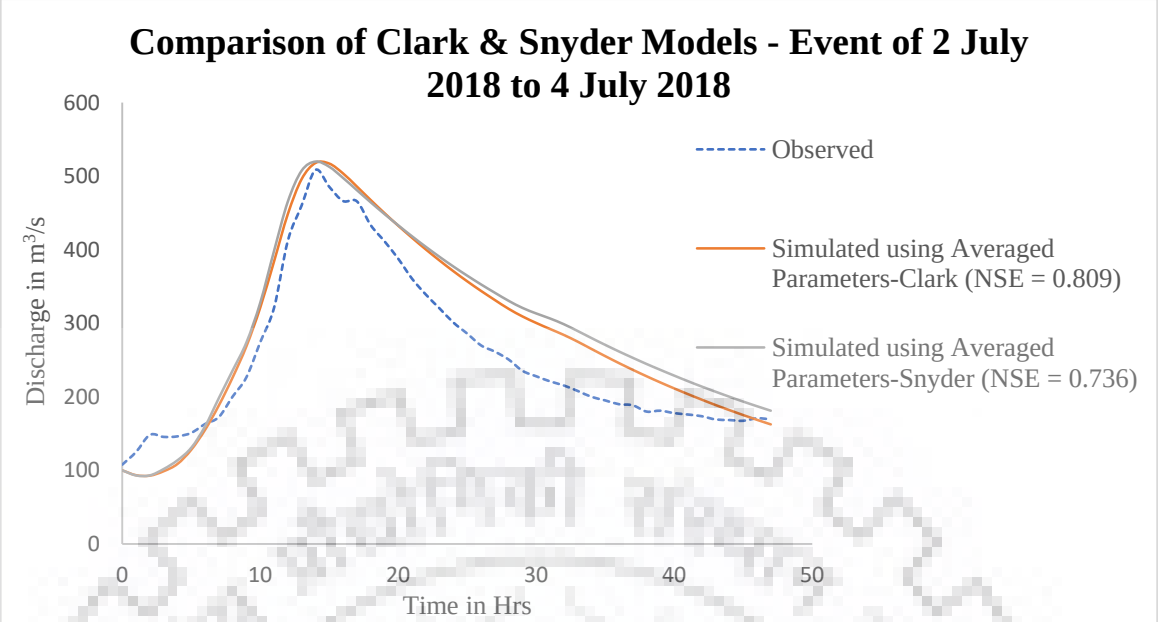

Figure 5.27 Comparison of Observed and Simulated Flood Hydrographs using Averaged Parameters of Clark and Snyder Models for event 2 July 2018 – 4 July 2018

Figure 5.28 shows the percent errors of three performance criteria such as percent error in peak, percent error in time to peak and percent error in discharge volume along with NSE values, computed during the calibration from the event 2 July 2018 – 4 July 2018 using two transform models. All the percent errors, computed from three different performance criteria of Clark and Snyder models have differ values which are shown in the figure. Furthermore, NSE value, which is an indicator of the overall performance of the transform model, is highest for the Clark model (NSE=0.809) whereas for the Snyder model (NSE=0.736)

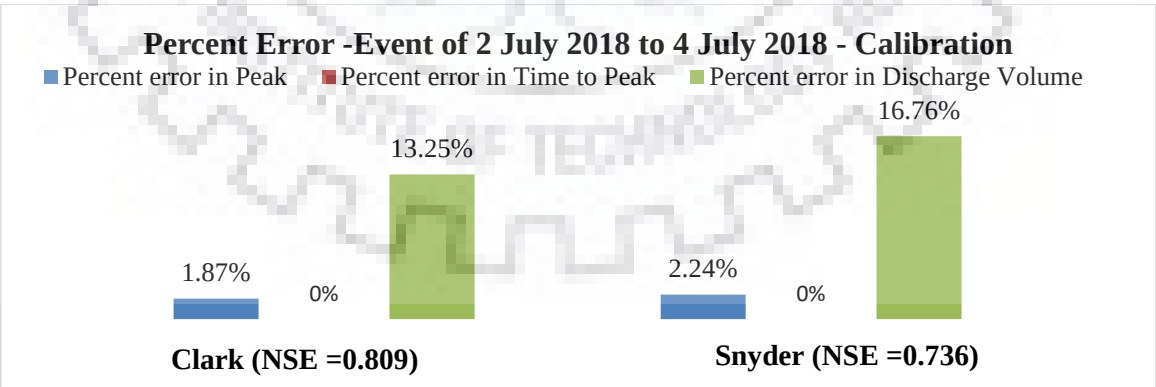

Figure 5.28 Comparison of Percent Errors of Clark and Snyder Models during Calibration using Averaged Parameters for event 2 July 2018 – 4 July 2018

Figure 5.29 shows the comparison of simulated flood hydrographs using representative parameters (averaged parameters) of the two transform model with the observed flood hydrograph for the event 12 August 2018 – 14 August 2018. From the figure, it is observed that the Clark UH transform model gave best performance with the NSE of 0.838 whereas the Snyder UH transform model have the performance with the NSE of 0.810.

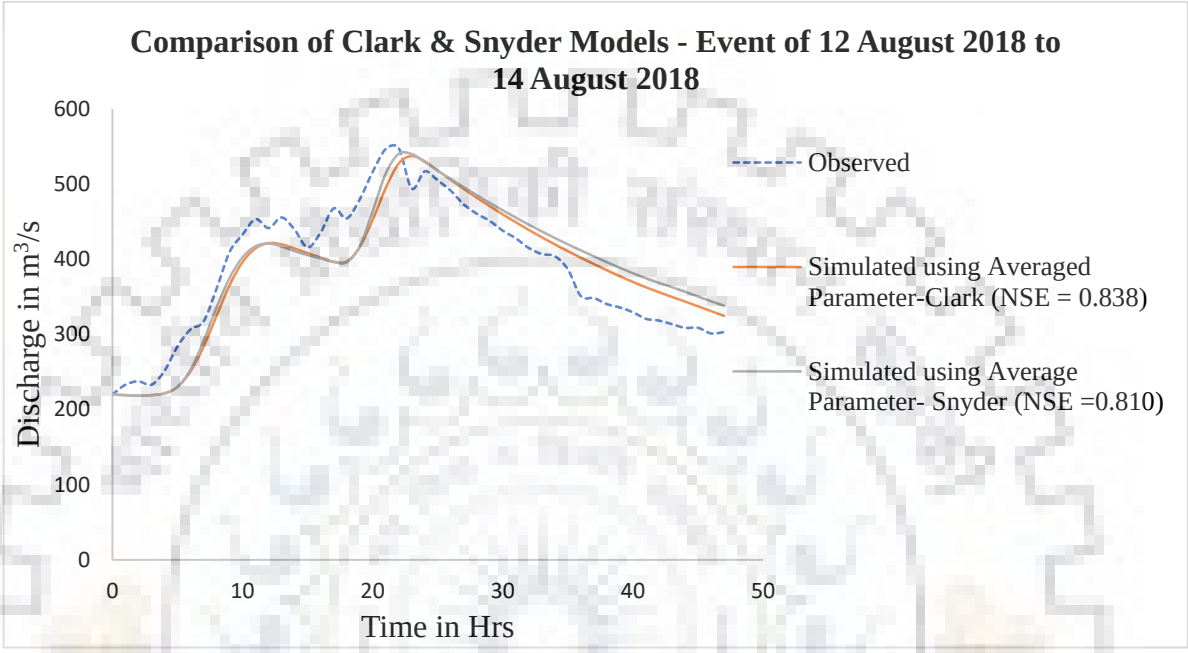

Figure 5.29 Comparison of Observed and Simulated Flood Hydrographs using Averaged Parameters of Clark and Snyder Models for event 12 August 2018 – 14 August 2018

Figure 5.30 shows the percent errors of three performance criteria such as percent error in peak, percent error in time to peak and percent error in discharge volume along with NSE values, computed during the calibration from the event 12 August 2018 – 14 August 2018 using two transform models. All the percent errors, computed from three different performance criteria of Clark and Snyder models have differ values which are shown in the figure. Furthermore, NSE value, which is an indicator of the overall performance of the transform model, is highest for the Clark model (NSE=0.838) whereas for the Snyder model (NSE=0.810)

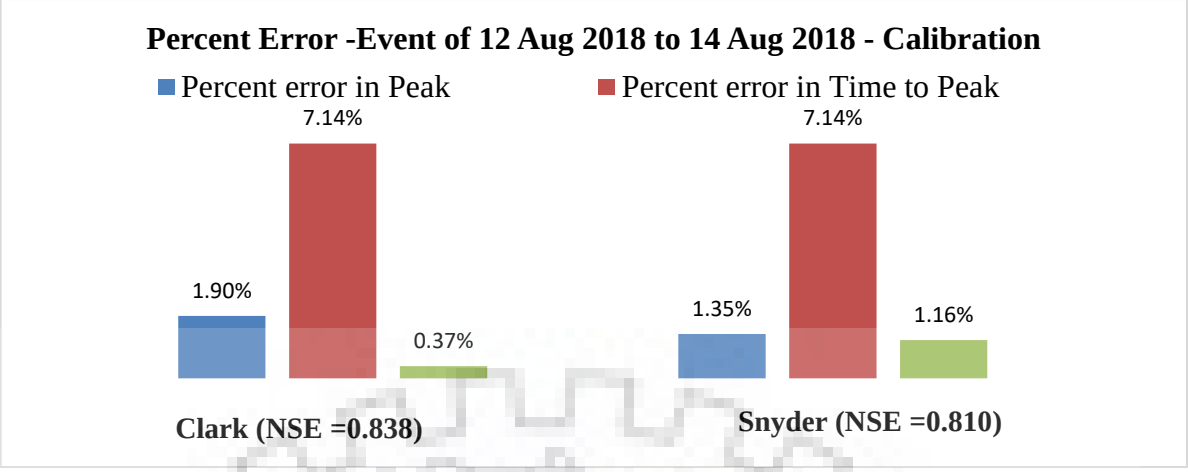

Figure 5.30 Comparison of Percent Errors of Clark and Snyder Models during Calibration using Averaged Parameters for event 12 August 2018 – 14 August 2018

5.6.4 Validation Of Clark UH Model- Event 11 July 2018 – 14 July 2018

The comparison of observed and simulated flood hydrograph at Bhorleni Gauging site using averaged parameters of Clark model for event 11 July 2018 – 14 July 2018 was considered for validation as shown in Figure 5.31. The NSE value obtained during the validation of Clark Model was 0.791.

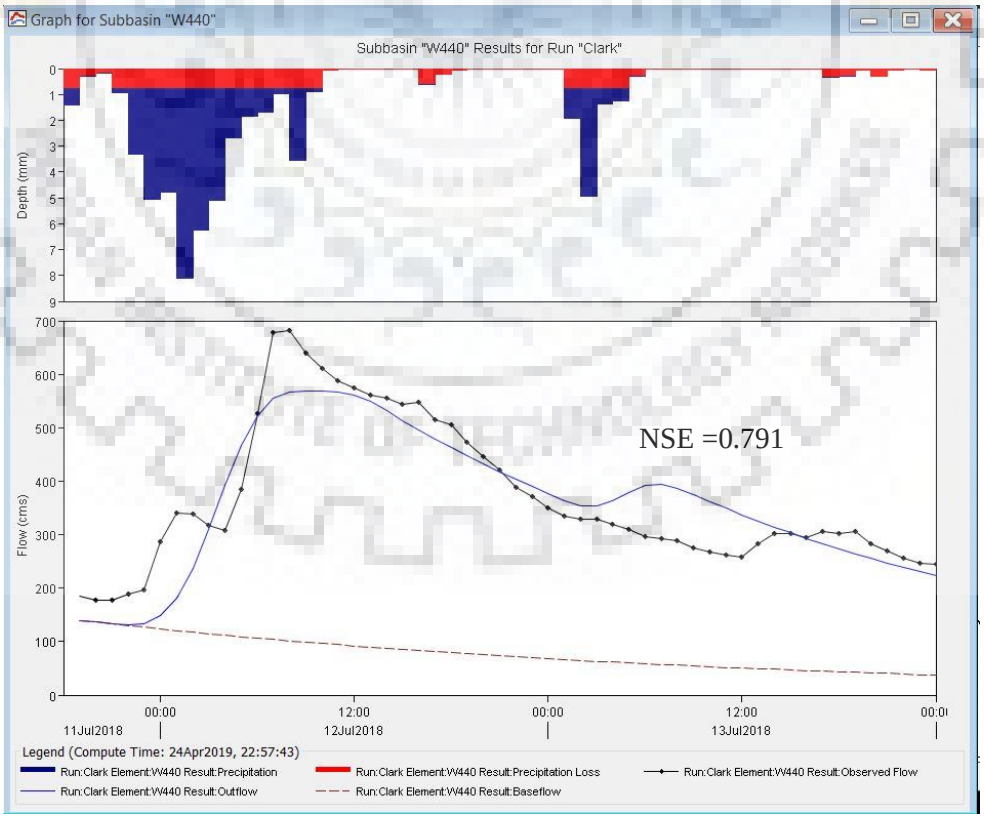

Figure 5.31 Comparison of Observed and Simulated Flood Hydrographs using Averaged Parameters of Clark Model for event 11 July 2018 – 14 July 2018 considered for validation

5.6.5 VALIDATION OF SNYDER UH MODEL- EVENT 11 JULY 2018 – 14 JULY 2018

The comparison of observed and simulated flood hydrograph at Bhorleni Gauging site using averaged parameters of Snyder model for event 11 July 2018 – 14 July 2018 was considered for validation as shown in Figure 5.32. The NSE value obtained during the validation of Clark Model was 0.755.

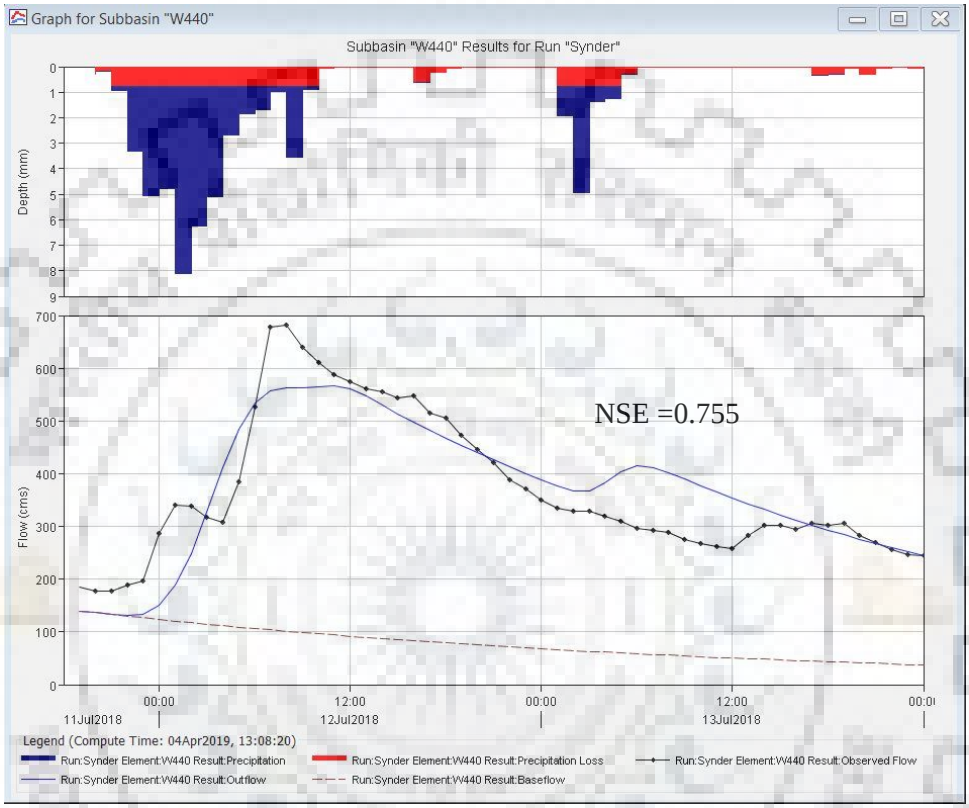

Figure 5. 32 Comparison of Observed and Simulated Flood Hydrographs using Averaged Parameters of Snyder Model for event 11 July 2018 – 14 July 2018 considered for validation

5.6.6 COMPARISON OF CLARK AND SNYDER MODELS DURING VALIDATION

Figure 5.33 shows the comparison of observed and simulated flood hydrographs of two transform models- Clark and Snyder models for the event 11 July 2018 – 14 July 2018 during validation. The performance of the Clark transform model was best as it had resulted in the highest NSE value of 0.791 whereas the performance of the Snyder transform model was found with the NSE of 0.755.

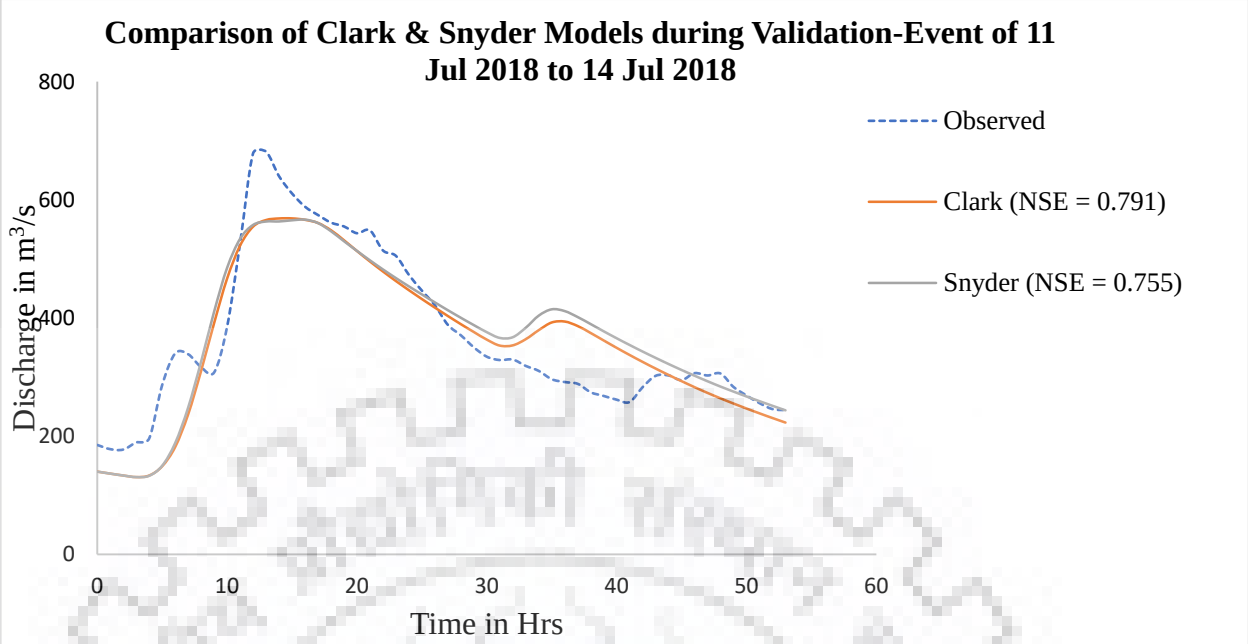

Figure 5.33 Comparison of Observed and Simulated Flood Hydrographs of Clark and Snyder Models during Validation considering for event 11 July 2018 – 14 July 2018

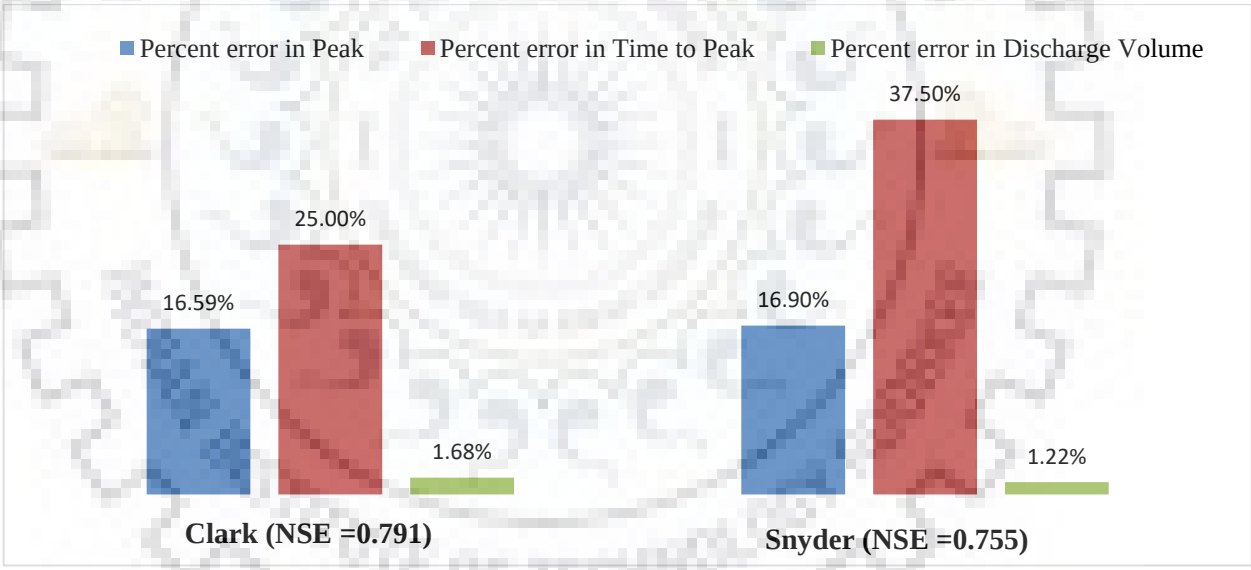

Figure 5. 34 Comparison of Percent Errors of Clark and Snyder Models during Validation considering for event 11 July 2018 – 14 July 2018

Figure 5.34 shows the percent errors such as percent error in peak, percent error in time to peak and percent error in discharge volume along with NSE values computed of during the validation considering for event 11 July 2018 – 14 July 2018 using Clark and Snyder Models. The percent error in peak and the percent error in time to peak in Snyder model is higher than the Clark model. Furthermore, NSE value which is an indicator of the overall

performance of the model, is highest for Clark model (NSE=0.791) whereas for Snyder model has value of NSE= 0.755.

From the calibration and validation results of Clark and Snyder models, Clark model is found to be the best performing model. Therefore, the unit hydrograph derived from Clark model is considered for further applications.

5.7 REAL TIME FLOOD FORECASTING

5.7.1 DEVELOPMENT OF UNIT HYDROGRAPH

The averaged parameters of Clark model, time of concentration Tc and storage coefficient is 5 hours and 27 hours respectively. The time-area relationship is given in Table 5.12 to develop the Clark unit hydrograph.

Tc =	5	Hr
R=	27	Hr
t =	1	Hr

Time (hrs)	Area At (sqkm)
0	-
1	313.48
2	371.10
3	384.65
4	410.07
5	215.20

Routing Coefficient, $C = 2t / (2R+t)$ (5.7.1)

$C = 0.036$

Routing Equation = $O_i = C I_i + (1-C) O_{i-1}$ (5.7.2)

$Ii = 0.2778 At / t$ (5.7.3)

Table 5. 12 Time-Area Relations to Develop Clark Unit Hydrograph

Time of travel in hrs	Area (At) in sqkm	Ii	C * Ii	(1-C) * Oi-1	Oi	Ordinates of 1 hr UH
0	-	0	0	0	0	0
1	313.48	87.085	3.135	0	3.135	1.568
2	371.10	103.09	3.711	3.022	6.733	4.934
3	384.65	106.856	3.847	6.491	10.338	8.536
4	410.07	113.917	4.101	9.966	14.067	12.203
5	215.20	59.783	2.152	13.561	15.713	14.89
6	-	0	0	15.147	15.147	15.43
7	-	0	0	14.602	14.602	14.875
8	-	0	0	14.076	14.076	14.339
9	-	0	0	13.569	13.569	13.823
10	-	0	0	13.081	13.081	13.325
11	-	0	0	12.61	12.61	12.846
12	-	0	0	12.156	12.156	12.383
13	-	0	0	11.718	11.718	11.937
14	-	0	0	11.296	11.296	11.507
15	-	0	0	10.889	10.889	11.093
16	-	0	0	10.497	10.497	10.693
17	-	0	0	10.119	10.119	10.308
18	-	0	0	9.755	9.755	9.937
19	-	0	0	9.404	9.404	9.58
20	-	0	0	9.065	9.065	9.235
21	-	0	0	8.739	8.739	8.902
22	-	0	0	8.424	8.424	8.582
23	-	0	0	8.121	8.121	8.273
24	-	0	0	7.829	7.829	7.975
25	-	0	0	7.547	7.547	7.688

26	-	0	0	7.275	7.275	7.411
27	-	0	0	7.013	7.013	7.144
28	-	0	0	6.761	6.761	6.887
29	-	0	0	6.518	6.518	6.64
30	-	0	0	6.283	6.283	6.401
31	-	0	0	6.057	6.057	6.17
32	-	0	0	5.839	5.839	5.948
33	-	0	0	5.629	5.629	5.734
34	-	0	0	5.426	5.426	5.528
35	-	0	0	5.231	5.231	5.329
36	-	0	0	5.043	5.043	5.137
37	-	0	0	4.861	4.861	4.952
38	-	0	0	4.686	4.686	4.774
39	-	0	0	4.517	4.517	4.602
40	-	0	0	4.354	4.354	4.436
41	-	0	0	4.197	4.197	4.276
42	-	0	0	4.046	4.046	4.122
43	-	0	0	3.9	3.9	3.973
44	-	0	0	3.76	3.76	3.83
45	-	0	0	3.625	3.625	3.693
46	-	0	0	3.495	3.495	3.56
47	-	0	0	3.369	3.369	3.432
48	-	0	0	3.248	3.248	3.309
49	-	0	0	3.131	3.131	3.19
50	-	0	0	3.018	3.018	3.075
51	-	0	0	2.909	2.909	2.964
52	-	0	0	2.804	2.804	2.857
53	-	0	0	2.703	2.703	2.754
54	-	0	0	2.606	2.606	2.655

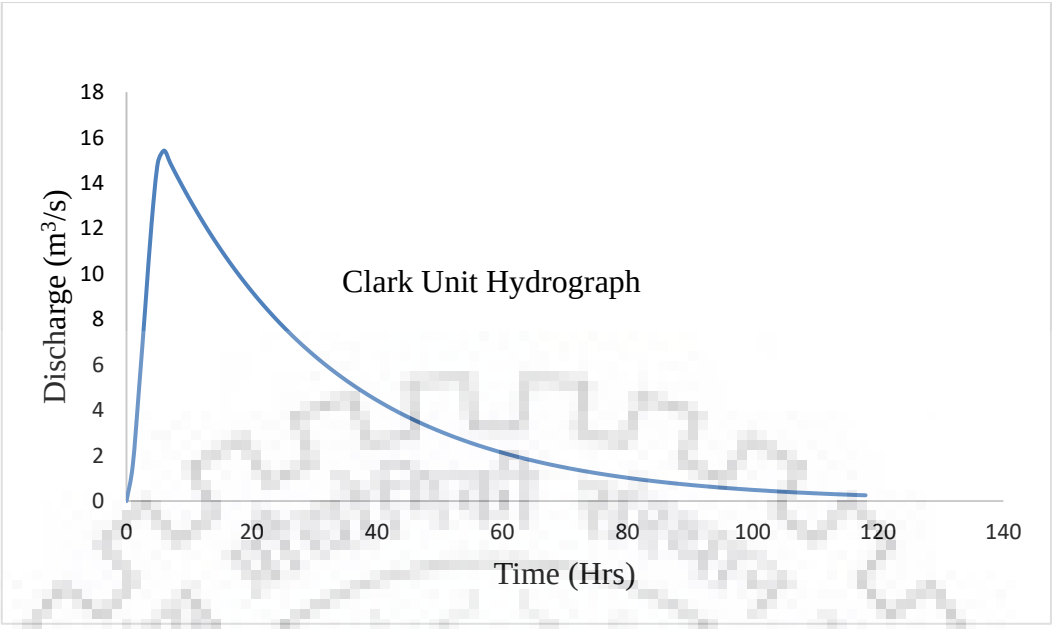

Figure 5.35 Clark Unit Hydrograph

5.7.2 FORECASTING OF FLOOD HYDROGRAPH

Flood forecasting is the prediction of water level occurring in rivers and flood plains. Flood hydrographs were forecasted for the event of 11 July 2018 – 14 July 2018 at each time step whenever a fresh observed rainfall values arrived at the forecasting station. For this purpose, excess rainfall computed for 11 July 2018 – 14 July 2018 event from HEC-HMS programme were convoluted with Clark Unit Hydrograph. Those forecasted flood hydrographs were developed for the successive 4 hours duration rainfall blocks of that event. The forecasted flood hydrographs for different lead times were computed as shown in Figure 5.36.

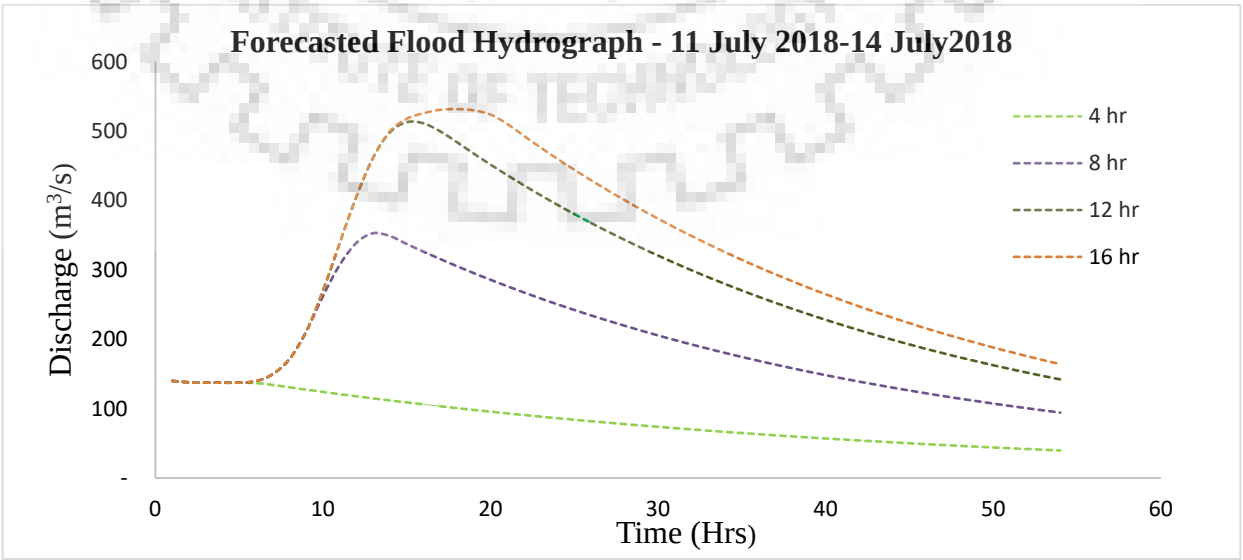

Figure 5.36 Forecasted Flood Hydrograph in real time for different lead times for event o11 July 2018 – 14 July 2018

Department of Hydrology and Meteorology, Nepal follows the reference given in Table 5.13 to take the precautionary steps over flood mitigation measures according to the flood extent. The risk assessment was carried out for the event of 11 July 2018 – 14 July 2018. The maximum water levels corresponding to the peaks of forecasted flood hydrograph were computed using the developed rating curve. The properties of forecasted flood hydrograph such as peak discharges, corresponding water levels, time to peaks and lead times along with the limits of risk are given in the Table 5.14.

Table 5.13 Risk Assessment at Bhorleni Maintained By Department Of Hydrology and Meteorology, Nepal

Water Level	Limits of Risk
4.2 m	Flood Warning Level
5 m	Danger Level

Table 5.14 Forecasted Flood Hydrograph Peak and Corresponding Water Levels, Time to Peak and Lead Time Along With Limits of Risks for Event 11 July 2018 – 14 July 2018

Duration of Excess Rainfall (Hr)	Peak Discharge (Qp) forecasted (m^3/s)	Water level forecasted (m)	Time to Peak (Hrs)	Lead Time (Hrs)	Limits of Risk
1	140.00	2.91	1	-	No Risk
2	140.00	2.91	1	-	No Risk
3	140.00	2.91	1	-	No Risk
4	140.00	2.91	1	-	No Risk
5	151.02	2.97	10	5	No Risk
6	209.79	3.27	11	5	No Risk
7	255.52	3.47	12	5	No Risk
8	352.64	3.81	13	5	No Risk
9	422.44	4.02	14	5	No Risk
10	477.53	4.17	15	5	No Risk
11	502.81	4.23	15	4	Flood Warning Level
12	512.58	4.25	15	3	Flood Warning Level
13	519.24	4.27	16	3	Flood Warning Level
14	519.66	4.27	16	2	Flood Warning Level
15	531.00	4.30	18	3	Flood Warning Level

Figure 5.37 shows the comparison of the forecasted flood hydrograph considering 16 hrs rainfall block and observed flood hydrograph for the event of 11 July 2018–14 July 2018. The forecasted flood hydrograph slightly fits the observed flood hydrograph. From the figure, it is observed that the forecasted flood hydrograph considering all the rainfall blocks is slightly closed agreement with the observed flood hydrograph. Thus, the forecasted flood hydrograph peaks and corresponding water levels considering the excess rainfall of different durations would provide very useful information for evacuating the people likely to be submerged during flood for the various forecasted water levels.

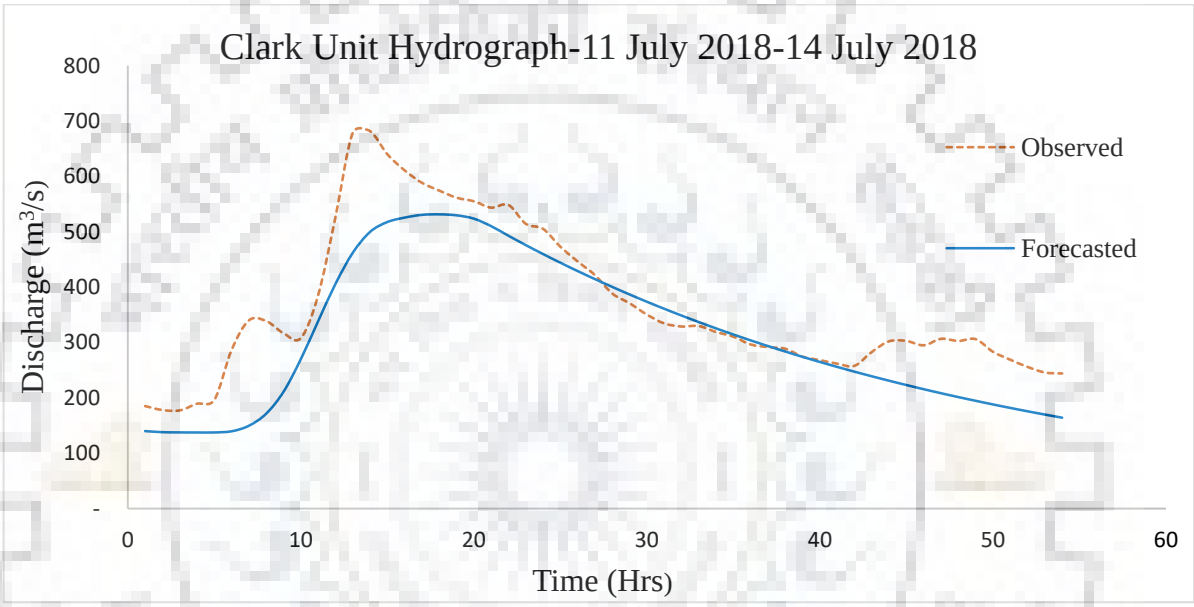

Figure 5.37 Comparison of Observed and Forecasted Flood Hydrograph considering 16 hrs. of excess rainfall using Clark UH for the event 11 July 2018 – 14 July 2018

5.8 UPDATING OF REAL TIME FLOOD FORECASTING

The updating of real time flood forecasting had been developed using the error prediction model of real time errors based on multiple linear regression method using the validated event of 111 July 2018 – 14 July 2018 which is shown in the Table 5.15 below. The forecasted Hydrograph is very close to observed hydrograph. The comparison of observed and updated hydrograph is shown in Figure 5.38.

Table 5.15 Updating of Real Time Flood Forecasting

Time in hrs	Computed Flood Hydrograph Ordinates m3/s	Observed Flood Hydrograph m3/s	Error, E_i (Observed-Computed)	E_{i-1}	E_{i-2}	E_{i-3}	E_i	Update Forecast (Computed + E_i)
0	0	0	0	-	-	-	4.70	4.70
1	140.00	185.10	45.10	-	-	-	1.52	141.52
2	137.99	178.00	40.01	45.10	-	-	67.60	205.59
3	137.57	177.30	39.73	40.01	45.10	-	16.65	154.22
4	137.46	189.30	51.84	39.73	40.01	45.10	36.88	174.34
5	137.51	196.10	58.59	51.84	39.73	40.01	53.77	191.28
6	139.62	286.40	146.78	58.59	51.84	39.73	51.97	191.60
7	149.60	339.90	190.30	146.78	58.59	51.84	183.71	333.32
8	171.43	338.70	167.27	190.30	146.78	58.59	165.17	336.60
9	210.91	316.80	105.89	167.27	190.30	146.78	118.43	329.34
10	269.82	307.80	37.98	105.89	167.27	190.30	63.25	333.07
11	338.32	385.00	46.68	37.98	105.89	167.27	12.45	350.77
12	405.59	526.00	120.41	46.68	37.98	105.89	71.01	476.60
13	461.81	678.50	216.69	120.41	46.68	37.98	150.47	612.28
14	499.59	681.70	182.11	216.69	120.41	46.68	227.13	726.72
15	517.52	640.00	122.48	182.11	216.69	120.41	105.57	623.09
16	525.48	610.80	85.32	122.48	182.11	216.69	83.18	608.66
17	530.48	588.40	57.92	85.32	122.48	182.11	73.31	603.79
18	531.40	574.30	42.90	57.92	85.32	122.48	47.22	578.62
19	529.66	561.50	31.84	42.90	57.92	85.32	38.26	567.93

20	523.64	555.00	31.36	31.84	42.90	57.92	26.57	550.21
21	510.08	543.50	33.42	31.36	31.84	42.90	31.44	541.52
22	492.76	548.40	55.64	33.42	31.36	31.84	31.13	523.90
23	475.91	514.40	38.49	55.64	33.42	31.36	62.71	538.62
24	459.68	505.20	45.52	38.49	55.64	33.42	15.42	475.11
25	444.07	473.00	28.93	45.52	38.49	55.64	50.92	494.99
26	428.96	446.40	17.44	28.93	45.52	38.49	12.67	441.63
27	414.42	421.60	7.18	17.44	28.93	45.52	14.08	428.50
28	400.34	388.40	-11.94	7.18	17.44	28.93	3.94	404.29
29	386.70	370.80	-15.90	(11.94)	7.18	17.44	(19.07)	367.63
30	373.59	350.40	-23.19	(15.90)	(11.94)	7.18	(9.84)	363.75
31	360.89	334.50	-26.39	(23.19)	(15.90)	(11.94)	(23.79)	337.09
32	348.68	328.80	-19.88	(26.39)	(23.19)	(15.90)	(22.86)	325.82
33	337.92	329.70	-8.22	(19.88)	(26.39)	(23.19)	(12.39)	325.53
34	332.47	318.90	-13.57	(8.22)	(19.88)	(26.39)	(2.22)	330.25
35	332.19	310.50	-21.69	(13.57)	(8.22)	(19.88)	(19.56)	312.63
36	334.37	296.40	-37.97	(21.69)	(13.57)	(8.22)	(22.50)	311.87
37	337.85	291.60	-46.25	(37.97)	(21.69)	(13.57)	(41.12)	296.73
38	338.07	288.60	-49.47	(46.25)	(37.97)	(21.69)	(40.52)	297.54
39	332.61	274.30	-58.31	(49.47)	(46.25)	(37.97)	(42.99)	289.62
40	323.83	268.10	-55.73	(58.31)	(49.47)	(46.25)	(56.21)	267.62
41	313.58	261.70	-51.88	(55.73)	(58.31)	(49.47)	(44.69)	268.90
42	302.86	257.80	-45.06	(51.88)	(55.73)	(58.31)	(44.52)	258.34

43	292.57	282.90	-9.67	(45.06)	(51.88)	(55.73)	(37.03)	255.55
44	282.62	302.10	19.48	(9.67)	(45.06)	(51.88)	11.41	294.03
45	272.97	302.70	29.73	19.48	(9.67)	(45.06)	23.21	296.18
46	263.62	294.90	31.28	29.73	19.48	(9.67)	22.54	286.16
47	254.67	306.60	51.93	31.28	29.73	19.48	25.10	279.77
48	246.00	302.70	56.70	51.93	31.28	29.73	58.61	304.62
49	237.70	306.00	68.30	56.70	51.93	31.28	46.01	283.72
50	229.57	283.20	53.63	68.30	56.70	51.93	66.26	295.83
51	221.79	268.90	47.11	53.63	68.30	56.70	34.19	255.98
52	214.25	255.90	41.65	47.11	53.63	68.30	42.88	257.13
53	206.96	245.80	38.84	41.65	47.11	53.63	35.81	242.77
54	199.99	244.00	44.01	38.84	41.65	47.11	34.63	234.62

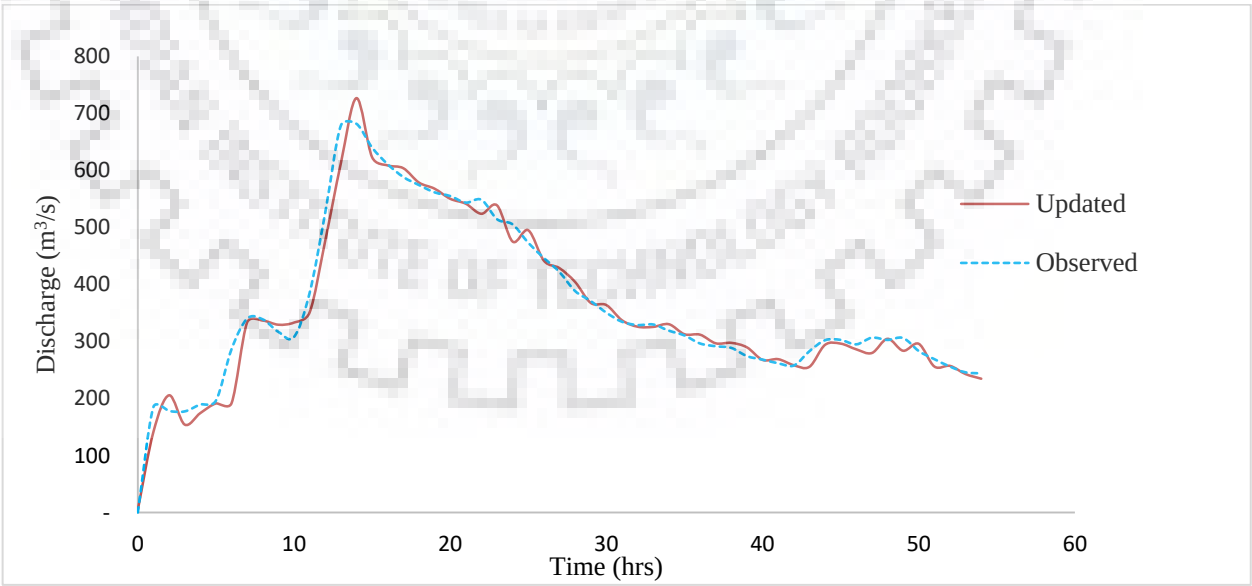

Figure 5.38 Comparison of Observed and Updated Forecasted Flood Hydrograph

5.9 LIMITATION OF THE STUDY

The limitations of the study are as follows:

1) In this study, data of 30-metre resolution for the digital elevation model (DEM) has been used. The results would be further improved if the higher resolution data are used during the simulation.

2) The quality of available data of stream flow and meteorology play very important role during simulation. The data contain some missing values which has been filled in during processing.

3) Out of eleven rain gauge stations, three rain gauge stations are outside the catchment. Furthermore, five stations are ordinary rain gauge (ORG) stations which have recorded daily rainfall values. The daily rainfall values for each ORG stations are converted into hourly rainfall values considering the representative SRRG stations.

4) The discharge data at the basin outlet is obtained from the rating curve but the rating curve used in the analysis is developed utilising the old historical records not from the recent records.

5) The transformation of sub basin runoff to the catchment outlet is carried out using HEC-HMS only which is based on the principle of unit hydrograph. It is recommended to use better non-linear models for the simulation of the flood hydrograph.

6) The study has been carried out considering a single basin. However, number of sub basins may be considered provided adequate data are available.

7) The error prediction model has been developed based on only one event. However, a comprehensive error prediction model need to be developed considering number of flood events. Subsequently, the real time flood forecast may be updated using such models for error prediction.

CHAPTER 6. CONCLUSION AND SCOPE FOR FUTURE STUDY

6.1 CONCLUSION

The relationship between rainfall and runoff is an important parameter for flood forecasting. So, the estimation of surface runoff in the basin due to precipitation and quantifying discharge at desired locations is important aspect of the flood forecasting and management plan. In some cases data are not available in Nepal with desired quantity and quality. For hourly discharge, real time data sets of at least hourly interval rainfall and water level are required. For an ungauged basin Synthetic unit hydrograph needs to be developed to get runoff hydrograph at the outlet. For this study, Clark method is used to get hourly discharge of the basin.

The following are the specific conclusions drawn from the results of this study:

1) ArcGIS software has been used for preparing the watershed delineation, digital elevation map, Thiessen polygon and isochrones map. For this purpose, the satellite data from the USGS web site has been downloaded on the 30-meter resolution.
2) In this study, HEC-HMS hydrological model is used to simulate rainfall-runoff process in Bagmati River Basin up to Bhorleni gauging site with a catchment area of about 1694.31 km^2.
3) HEC-GeoHMS software has been used to set up the basin model development. The software can prepare basin maps and provide the physiographic and some important geomorphological characteristics of the basin. The basin maps are taken as the input for HEC-HMS programme during the simulation runs.
4) The sensitivity analysis has been carried out to identify the initial parameters values of Clark and Snyder transform models. In Clark model; parameters optimization is carried out to optimize the parameters, Time of concentration (T_c) and Storage Coefficient (R). Similarly, in Snyder model parameters Peaking Coefficient C_p and Standard Lag (T) are optimized. The models are calibrated with two historical flood events and validated with one historical flood event by comparing observed and simulated discharge hydrographs at the Bhorleni gauging site.

5) During calibration and validation; the performance of the Clark and Snyder transform models is compared based on the overall performance criteria which include Nash-Sutcliffe efficiency (NSE) criteria and some error functions such as percent error in peak, percent error in time to peak and percent error in discharge volume. Based on the comparison, it is found that the performance of the Clark model is better than the Snyder model. The NSE obtained from the Clark model is found to be 0.791 whereas it is 0.755 for Snyder model.
6) The Clark transform model has been applied for the development of unit hydrograph of the Bagmati River Basin up to Bhorleni gauging site to forecast the flood of 11 July 2018 - 14 July 2018 event, which has been considered for the validation. The unit hydrograph, thus obtained, is used to forecast the floods in real time starting it from the first block of hourly rainfall and considering the subsequent hourly rainfall since the beginning of the storm at each hour. The limits of risk assessments are identified based on the criteria given by the Department of Hydrology and Meteorology, Nepal. The forecasted flood hydrographs would be very much useful for providing the advance information for the flood management planning and implementation of the evacuation of people from the flood affected area to the safer places minimising the losses of lives and properties.
7) The forecasted flood hydrographs of the event 11 July 2018 - 14 July 2018 considering different blocks of rainfall have been compared with the observed flood hydrograph of that event. During the comparison, it is observed that the forecasted flood hydrographs somewhat matches with the observed flood hydrograph. However, criteria of limits of risk started gently and showed flood warning level with the increase of lead times which can be considered for taking advance actions by the concerned authorities as per the limits of risk.
8) Using the developed error prediction model based on multiple linear regression approach, the real time flood forecast has been updated. It is found that the updated flood forecast has been significantly improved and found to be very close to the observed flood hydrograph.

6.2 SCOPE FOR FUTURE STUDY

1) Study need to be taken up with adequate and good quality hydro meteorological and hydrological data base for a greater accuracy in the results.
2) Number of flood events need to be considered for calibration and validation of the HEC-HMS model. The validated model may be applied for forecasting the floods and corresponding water levels in real time and those may be tested over several historical flood events before adopting the methodology.
3) For the prediction of the errors, a study needs to be taken up considering the various structures for the error prediction models. A suitable structure for the error prediction model may be selected for updating the flood forecast.
4) A comparative study needs to be taken up to judge the performance of various methods by comparing the results of the model parameters updating as well as the error prediction model. Multiple error modeling like Fuzzy, ANN etc. needs to be taken up to improve the flood forecast.

REFERENCES

1) Babel M.S. & Agarwal A., (2013) "Climate Change and water resources in the Bagmati River Basin, Nepal"; article in Theoretical and Applied Climatology.

2) Baral M. (2008), "Rainfall Runoff Modelling and Inundation Analysis of Bagmati River at Terai Region of Nepal"; International Centre for Water Hazard and Risk Management, Tsukuba, Japan

3) Choudhari K., Panigrahi B. & Paul J.C (2014), "Simulation of rainfall runoff process using HEC-HMS model for Balijore Nala watershed, Odisha, India"; International Journal of Geomatics and Geosciences, 5(2), 253

4) Clark C.O., (1945). "Storage and the Unit Hydrograph"; Transactions, ASCE, 110; 1419-1446

5) Dhital Y.P, Qiuhong T. and Jiancheng S. (2013), "Hydroclimatological changes in the Bagmati River Basin, Nepal", Journal of geographical Science Vol.23, No.4, 612-626

6) Dilley M., Chen R.S, Deichmann U., Lerner-Lam A.L, Arnld M. with Agwe J., Buys P., Kjekstad O., Lyon B. and Yetman G.(2005), "Natural disaster hotspots: a global risk analysis"; International Bank for Reconstruction And Development/ The world Bank and Columbia University, Washington, DC

7) Dr. K.R. Arora (Reprint 2016 published by A.K Jain), "Irrigation, Water Power and Water Resources Engineering".

8) DWIDP (2006), "Disaster Reviews from 1983-2006"; Department of Water Induced Diaster Prevention, Lalitpur, Nepal.

9) Garrote L., & Bras R. L. (1995), "A distributed model for real-time flood forecasting using digital elevation models"; Journal of Hydrology, 167(1), 279-306.

10) Gautam, N.P. (2015), "Hydrological Modelling with HEC-HMS in Different Channel Sections in Case of Gandaki River Basin"; Global Journal of Research in Engineering, 15(2)

11) Huang J., Chan Y. and Lee K. (2015) "Real-Time Flood Forecasting System: Case Study of Hsia-Yun Watershed, Taiwan"; Journal of Hydrologic Engineering.

12) Jaina S.K, Manib P, Jaina S.K, Prakashc P. et al. (2018), "A Brief review of flood forecasting techniques and their applications"; International Journal of River Basin Management, 1-16

13) K Subramanya (Reprint Edition, 2015) Engineering Hydrology published by Mc Graw Hill Education (India)

14) Knebl M., Yang Z.L., Hutchison K. et al. (2005), "Regional scale flood modeling using NEXRAD rainfall, GIS, and HEC-HMS/RAS": A case study for the San Antonio River Basin Summer 2002 storm event, Journal of Environmental Management, Vol:75, Pages: 325-336

15) Manjan S.K & Aggarwal S. (2014), "Hydrological modeling of Bagmati River Basin, Nepal"; International Journal of Current Engineering and Technology Vol.4, No.6

16) Manoj N., Kurian C. & Sudheer K.P (2016), "Development of a flood forecasting model using HEC-HMS" paper published on National Conference on Water Resourcse & Flood Management, SVNIT, Surat.

17) Nash, J.E. & Sutcliffe J.V. (1970). "River flow forecasting through conceptual through conceptual model Part I-A discussion of principles"; Journal of hydrology, 10(3), 282-290.

18) Serban, P. (Year 1991), "Hydrological Forecasting and Updating Procedures", World Meteorological Organization, Geneva, Switzerland.

19) Singh R.D (Year 2007), "Real Time Flood Forecasting- Indian Experiences" Journal: Modelling in Arid and Semi-Arid Areas

20) UNDP, 2004," Reducing disaster risk: A Challenge for development", United Nations

21) US Army Corps of Engineers (1995). "The hydrological modelling system (HEC-HMS)"; Design and development issues, Technical paper No.149

22) US Army Corps of Engineers (2009). "HEC-Geo-HMS Geospatial Hydrological Modeling Extension, user's manual version 4.2",

23) US Army Corps of Engineers December (2013). "Hydrologic modelling system HEC-HMS, user's manual version 4.2.1"

24) W.Resources (2018), "Standard Operating Procedure (SOP) For Flood Early Warning System In Nepal", Published by GoN/Ministry of Energy, Water Resources and Irrigation/Department of Hydrology and Meteorology, Kathmandu, Nepal.

25) World Meteorological Organization (2011), "Manual on flood forecasting and warning".

26) Xiong L. and Connor K.M.O (2002), “Comparison of four updating models for real-time river flow forecasting”, Hydrological Sciences Journal Vol.47, No.4, 621-639.